RGO/N, Co-TiO$_2$ Nanocomposites for Efficient Photodegradation of Methyl Orange

Name: Aroosa Javed

Reg. No. 00000117207

A thesis submitted in partial fulfillment of the requirements for the degree of Master of Science in Chemistry

Supervised by: Prof. Dr. Habib Nasir

Department of Chemistry

School of Natural Sciences (SNS)

National University of Sciences and Technology (NUST)

H-12, Islamabad, Pakistan

2017

National University of Sciences & Technology

MS THESIS WORK

We hereby recommend that the dissertation prepared under our supervision by: AROOSA JAVED, Regn No. 00000117207 Titled: RGO/N,Co-TiO2 Nanocomposites for Efficient Photodegradation of Methyl Orange be accepted in partial fulfillment of the requirements for the award of **MS** degree.

Examination Committee Members

1. Name: DR. ZAHIDA MALIK   Signature:

2. Name: DR. AZHAR MAHMOOD   Signature:

3. Name: Signature:

External Examiner: DR. ABDUL MATEEN   Signature:

Supervisor's Name: PROF. HABIB NASIR   Signature:

Head of Department

18-11-17

Date

COUNTERSINGED

Date: 18/11/17

Dean/Principal

THESIS ACCEPTANCE CERTIFICATE

Certified that final copy of MS thesis written by **Ms. Aroosa Javed**, (Registration No. **00000117207**), of **School of Natural Sciences** has been vetted by undersigned, found complete in all respects as per NUST statutes/regulations, is free of plagiarism, errors, and mistakes and is accepted as partial fulfillment for award of MS/M.Phil degree. It is further certified that necessary amendments as pointed out by GEC members and external examiner of the scholar have also been incorporated in the said thesis.

Signature: _____

Name of Supervisor: Prof. Habib Nasir

Date: _____ 18-11-17 _____

Signature (HoD): _____

Date: _____ 18-11-17 _____

Signature (Dean/Principal): _____

Date: _____ 18/11/17 _____

Dedicated to my loving Parents and Siblings for their prayers, love, faithfulness and support

Acknowledgements

Abstract

In textile industries, different types of dyes are used widely. Widespread use of these dyes causes surface and ground water contamination. This contaminated water is harmful for the human beings and other organisms as well. Therefore, treatment of this contaminated water is really important. These dyes can be removed from waste water by using biodegradation but this method doesn't remove these dyes completely. Photodegradation has proved really successful in converting these toxic compounds to non-toxic or less toxic compounds e.g. CO_2 and H_2O. In this work, nanoparticles of un-doped and doped TiO_2 were synthesized by sol-gel method. For the synthesis of undoped TiO_2 nanoparticles, TTIP, 2-propanaol and distilled water were used. Whereas, for nitrogen and cobalt doping, urea and cobalt nitrate were used along with TTIP, 2-Propanol and distilled water. The ratio of TTIP: Urea was 1:3 for all doped and co-doped samples and cobalt nitrate was taken in four different concentrations i.e. 0.5%, 1%, 2%, 6% and 7%. The samples were characterized by SEM, EDX, XRD, UV-Vis DRS and BET. From SEM analysis the information about the morphology and particle size of nanoparticles was obtained. EDX gave information about elemental composition of all the synthesized catalysts. XRD results confirmed the presence of anatase phase and tetragonal structure in all the synthesized catalysts. From UV-Vis DRS data, band gap was calculated by Tauc plot and BET analysis helped in the determination of surface area. Photodegradation of methyl orange was carried out by using undoped TiO_2, N-TiO_2 and N, Co-TiO_2 nanoparticles. The photocatalytic activity of nitrogen, cobalt co-doped catalysts was higher than undoped and nitrogen doped TiO_2. The best catalyst was than selected for the synthesis of nanocomposite with graphene oxide. Graphene oxide was synthesized by Hummers' method and nanocomposite was synthesized by hydrothermal method. The nanocomposites were synthesized in three different ratios of N, Co-TiO_2: GO which were 1:1, 1:1.5 and 1:2. These nanocomposites were than used for photocatalytic degradation of methyl orange. Nanocomposite with 1:1.5 showed best results as compared to other two nanocomposites. Highest degradation efficiency was achieved with NC-2 that was 93%.

List of Abbreviations

BET (Brunauer-Emmett-Teller)

DRS (Diffuse Reflectance Spectroscopy)

EDX (Energy Dispersive X-ray Spectroscopy)

FT-IR (Fourier Transform Infrared Spectroscopy)

GO (Graphene Oxide)

RGO (Reduced Graphene Oxide)

SEM (Scanning Electron Microscopy)

TTIP (Titanium Tetra Isopropoxide)

XRD (X-Ray Diffraction)

Table of Contents

List of Figures

List of Tables

1. Introduction

1.1. Nanoscience and nanotechnology

Nanoscience is a combination of two words "nano" and "science". Nanoscience includes the study of structures and materials on nanoscale. Properties and phenomenon associated with nanoscale materials is also studied in nanoscience. Nanotechnology is defined as "The manipulation of matter on an atomic and molecular level". Nano is a Greek word which is used as a prefix by the scientists to mean one billionth of a unit of measure e.g. nanosecond, nanometer etc. Properties of materials change at nanoscale which includes reactivity, optical properties, electrical properties, physical properties and chemical properties [1].

1- **Optical properties**: Optical properties of smaller particles are different than bulk materials, this is because light is absorbed and reflected differently by particles of different sizes so they can have different colors e.g. bulk sized gold is yellow in color, whereas the color of nanosized gold is red. Similarly large ZnO particles are able to scatter visible light but nanosized ZnO particles are smaller than wavelength of visible light so they cannot scatter it. Large ZnO particles are white in color but nanosized ZnO particles appear clear [1].

2- **Electrical Properties:** Electrical properties can be explained by the example of nanotubes. Long and thin cylinders of carbon are called nanotubes which are highly flexible, have unique electrical properties and are much stronger than steel. Their electrical properties are changed by a change in diameter, number of walls and twist [1].

3- **Physical properties**: Decreasing particle size to nanoscale causes a drastic decrease in melting point. This drastic decrease in melting point is because of the reason that the nanomaterial's have much larger surface to volume ratio than bulk materials [2].

4- **Chemical properties of the materials:** Reactivity of nanoparticles is higher than bulk materials as they have much exposed surface area than bulk materials. Following are some important features regarding chemical properties of nanoparticles [2].

i. Nanoparticles have 50% of all the atoms on their surface so their electrical properties do not depend on solid state bulk phenomenon.

ii. As the nanomaterial's have a large proportion of atom present on their surface so energy of atoms present in nanomaterial's is much higher than the atoms present in bulk materials.

iii. Surfaces and interfaces of nanomaterial's can easily attract highly charged species and impurities as they have much higher surface area and in this way chemical nature of the surfaces of nanoparticles are changed than bulk materials.

Two approaches are used to synthesize nanomaterials

a) **Top down approach:** In this approach, nanomaterials are obtained by milling or etching of bulk materials. Different techniques are used for top down fabrication in nanotechnology which includes mechanical and chemical fabrication techniques. Nanolithography is a commonly used top down approach. In nanolithography, the required material is protected by a mask and exposed material is etched away [3].

b) **Bottom up approach:** In this approach atoms or molecules self-assemble to form nanomaterials. This approach is used to obtain nanomaterials with less number of defects. On the other hand by using top down approach, there are chances of the development of internal stress along with contaminations and surface defects [3].

1.2. Classification of nanomaterials

Nanomaterial's are classified on the basis of number of dimensions which do not lie in the nanometer range (<100 nm) [4]. An essential quality of quantum mechanics which is also known as quantum confinement is shown by nanostructures. Quantum confinement means the trapping of electrons in a small area. A typical way which is used to classify the nanomaterials is on the basis of dimensions. Nanomaterials are classified into three classes on the basis of dimensions.

0-Dimensional Materials: 0-Dimensional materials have size range greater than 100 nm and their nano-dimensions can be measured in all the three directions. Examples of 0-Dimensional nanomaterial's include nanoparticles and quantum dots etc. [4].

Nanoparticles can be:

- Either amorphous or crystalline (single or polycrystalline)
- Can consist of single or multiple elements
- Can show different shapes

Quantum dots are semiconductor particles with their size lying in the nanometer range. When light is applied to these quantum dots, they can emit light of different frequencies which can be varied by varying their size and shape and can be used for different applications [5].

1-Dimensional materials: The materials having one dimension outside the nanoscale range are 1-Dimensional materials. They have needle-like shape. Common examples of these materials include nanotubes, nanowires and nanorods. These materials can have length of several micrometers but their diameter lies in the nanometer range. These materials can be [5]:

- Amorphous or crystalline (single or polycrystalline)
- Chemically pure or can have some impurities

Nanotube is a 1-Dimensional nanostructure having a hollow core

Nanofibers are 1-Dimensional nanomaterials which are amorphous and nonconductive usually.

Nanowire is a 1-Dimensional nanomaterial which is crystalline in nature and it can be metallic or semiconducting.

2-Dimensional materials: These materials have two dimensions out of nanometer range. They have plate-like shape. Common examples include nanofilms, nanocoatings and nanolayers. These materials can have large area but their thickness always lies in the nanometer range. These materials can be

- Amorphous or can be crystalline
- Used as a single or multilayer structure
- Deposited on a substrate

3-Dimensional materials: These materials have all the dimensions outside the nanometer range. They are also called bulk nanomaterials. These materials have nanocrystalline structure composed of different arrangements of nanosized crystals which arrange themselves in different directions. These nanomaterials can contain dispersed nanoparticles, nanotubes and multi-nanolayers. These materials can be

- Amorphous or crystalline
- Chemically pure or can have some impurities

1.3. Applications of nanomaterials

Nanomaterials are used for different applications as they have astonishing physical, chemical and mechanical properties. Fig 1.1 gives an overview of some fascinating applications of nanomaterials.

Antibacterial	Biomedicine	Sensors	Batteries
Displays	Photoelectronics	Agriculture	Solar cells
Environment	Catalysis	Thermoelectronics	Tissue enginnering
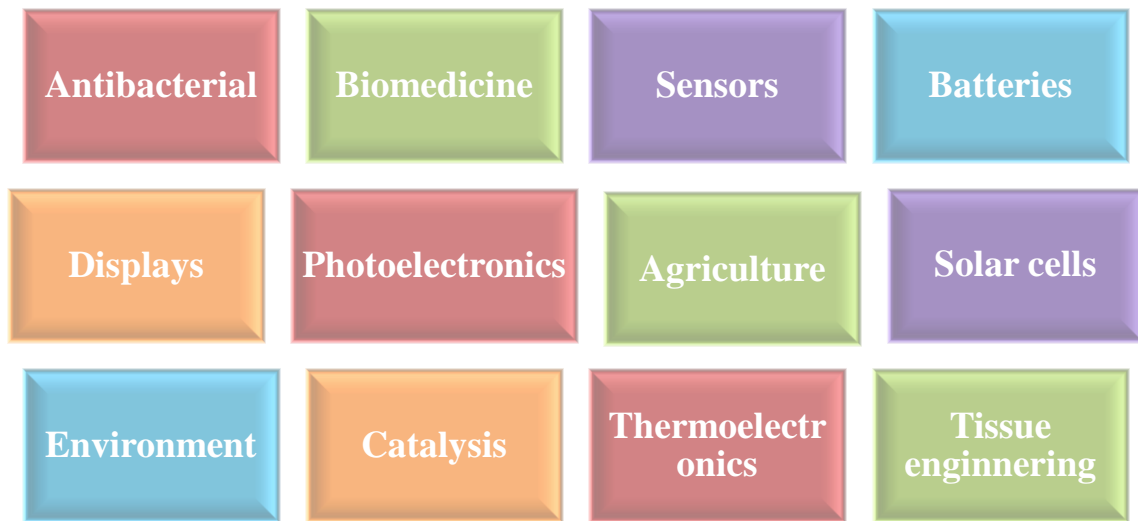
Figure 1.1 Applications of nanomaterials

These unique applications of nanomaterials are because of their peculiar physical properties, high surface area and small size. The environmental applications of these nanomaterials are quite significant. These nanomaterials play a very important role in preventing the release of different chemicals from laboratories, industries and other places which can be hazardous. Nanocrystalline materials are used in air filtration technologies.

These nanomaterials are also used in controlling different inorganic and organic contaminants in water [6].

Nanomaterials have also effects on plant germination and growth so they are also used for agricultural applications. The effects of bulk TiO_2 and nano-TiO_2 on the growth of spinach seeds has been studied by Zheng [7]. Plants which were produced from seeds that were treated with nano-TiO_2 had 73% more dry weight and their photosynthetic rate was also three times higher. It was also found that growth rate of spinach seeds had inverse relation with materials size which means that smaller nanomaterials cause better germination.

Because of successful development of nanomaterials, they are also used in medicine and biology leading to the development of nanobiotechnology. Research in nanotechnology has grown explosively in the last two decades. Nanobiotechnology is a new emerging field which combines nanotechnology and biotechnology. Nanomaterials which include nanoparticles and nanofibers etc. have their properties different from bulk materials, so they are used in many biological applications which include biosensing, anticancer therapy and biological separation etc. These nanomaterials can be used to study complex biological processes as they have unique properties [6].

When nanopowder is added in production of alloys and steel, their mechanical properties are improved. Some coatings have been developed by using TiO_2 nanoparticles and polymer binder which prevent the surfaces from getting wet with water and oil etc. The use of carbon nanotubes in electronics is becoming common. They cannot only replace the transistors but can also increase the mechanical and optical properties of electronics, making them more flexible. Nanomaterials are also used in manufacturing highly efficient and low cost solar cells.

1.3.1. Photocatalytic applications of nanomaterials

Physical and chemical properties of nanomaterials change when their size approach to nanometer range and these properties also change with a change in shape of these nanomaterials. Reduction in particle size also causes high surface area which is very important to build TiO_2 devices. TiO_2 is the most promising photocatalyst used now days to overcome environmental pollution. It is also expected that through effective utilization of solar energy it can also overcome energy crisis [8]. TiO_2 is used in photocatalytic

oxidation processes to bring about the degradation of organic pollutants in air and water. TiO_2 is chemically stable having a flat band potential, as a result redox reactions can be induced in it without using external potential. Moreover TiO_2 is low cost and is abundantly available. However TiO_2 doesn't absorb the visible light so it cannot utilize the solar light effectively. To extend it's absorption into the visible region it can be doped with different elements which reduce it's band gap, lowering the energy required for the excitation of electrons. Another factor which limits its efficiency for photocatalytic applications is rapid recombination of electrons and holes, so to overcome this TiO_2 is combined with some suitable materials e.g. graphene oxide so that electron hole recombination can be prevented and by using these electrons and holes, oxidation and reduction of organic pollutants can be carried out [9].

1.4. TiO$_2$ nanostructured materials

Titanium is a transition metal having atomic number 22. This metal is light in weight, strong and corrosion resistant. Most commonly used compound of this metal is TiO_2. This powder is commercially produced since the start of 20th century so it has been used as a pigment in toothpaste, sunscreens and paints etc. In 1972, the phenomenon of water splitting was studied by Fujishima and Honda on TiO_2 electrode in presence of UV light [10]. Since then a lot of research has been carried out to use TiO_2 for different applications e.g. photocatalysis, photoelectrochromics, photovoltaics and sensors.

1.5. Background of TiO$_2$

Because of promising applications of semiconductor photocatalysis in environmental purification and solar energy conversion, it has attracted great attraction and a lot of research has been carried out on it. Semiconductors which include TiO_2, ZnO, WO_3 and CdS have a unique electronic structure comprising of a filled valence band and empty conduction band, so these semiconductors can be used as photocatalyst in different chemical transformations induced by light. When a photon of light having energy greater than or equal to the band gap energy (E_g) of semiconductor falls on it, it causes excitation of electron from valence band to conduction band as a result holes are created in the valence band. The recombination of these electron and holes will lead to release of input

6

energy in the form of heat. On the other hand, these charge carriers can be used for photodegradation. In the last 10 years, research has been carried out to use these nanostructured materials as building blocks for construction of light-harvesting assemblies [11].

TiO_2 is the most commonly used photocatalyst as it is:

1. Non-toxic
2. Stable under sunlight
3. Commercially available and has an appropriate electronic structure

Different morphologies of TiO_2 have been reported which include nanowires, nanoparticles, nanofibers and nanotubes etc. along with that it's composite with different materials have also been prepared. Because of effective utilization of solar energy TiO_2 will not only overcome energy crisis but can also meet environmental challenges.

1.6. Applications of TiO_2 nanoparticles

TiO_2 is one the most commonly available nanomaterials having fascinating applications. TiO_2 is the most important photocatalyst as it has strong oxidizing power [11, 12]. Some applications of TiO_2 nanoparticles are shown in Figure 1.2.
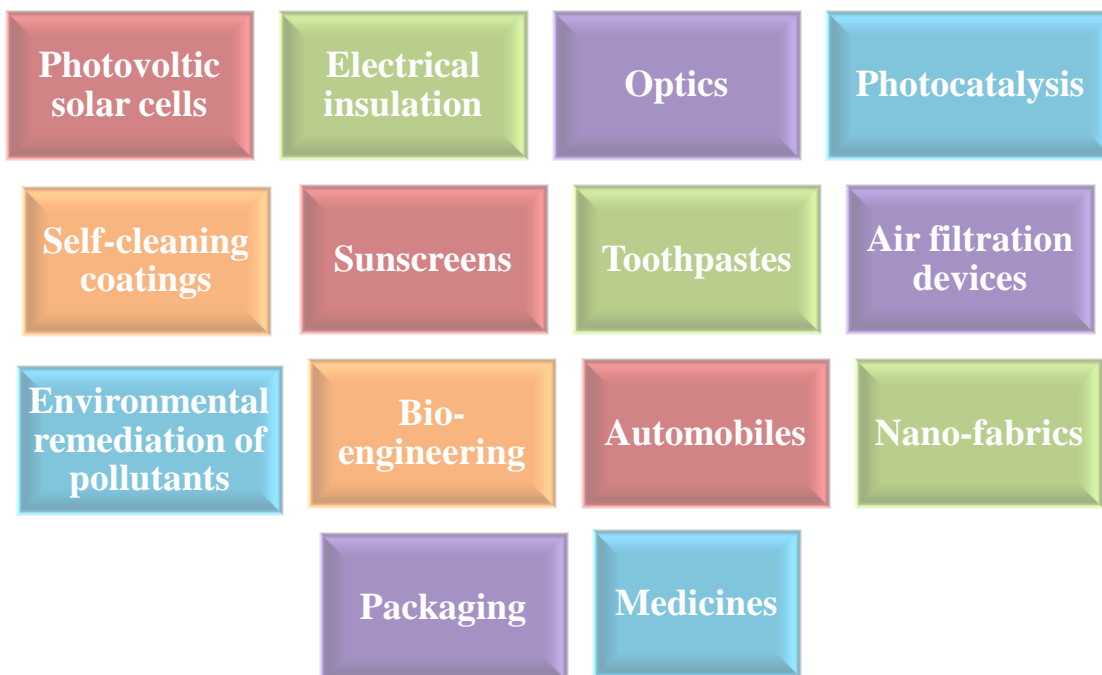
Figure 1.2 Applications of TiO_2 nanoparticles

TiO$_2$ nanaoparticles are also used in treatment of contaminated water . Some important applications of TiO$_2$ nanoparticles have been discussed in detail below.

1.6.1. Application in solar water splitting

After the discovery of splitting of water on TiO$_2$ electrode, research has been carried out to study the properties and applications of TiO$_2$ by using UV radiations [13]. This splitting of water by using TiO$_2$ is carried out by using solar light. Under UV irradiations, electrons get excited to conduction band and holes are created in the valence band. These charge carriers can bring about redox reactions. Water is oxidized to oxygen by holes and electrons reduce water to hydrogen leading to overall splitting of water.

1.6.2. Application in photovoltaics

Dye-sensitized solar cell (DSSC) use electrodes of nanocrystalline TiO$_2$ [13, 14] which are placed in a redox electrolyte. The structure and properties of TiO$_2$ electrodes affect the performance of DSSC to a greater extent e.g. the adsorption of dye is increased with the mesoporosity and crytallinity of TiO$_2$ electrode [15]. Electron density is increased by using TiO$_2$ nanotubes which increases the efficiency of solar cells [16]. The efficiency was increased by the use of doped TiO$_2$ electrodes as the absorption is shifted to visible region which increases the photo-induced current [17].

1.6.3. Application as a catalyst support or promoter

TiO$_2$ is used in catalytic activity as it increases the surface area of catalyst. Reactivity and selectivity of the catalyst is changed due to the interactions between the catalyst and TiO$_2$ [18]. The catalytic activity of V$_2$O$_5$ supported on TiO$_2$ in oxidizing the hydrocarbons and reducing the nitric oxides was found to be higher than unsupported V$_2$O$_5$ [19].
Although TiO$_2$ cannot be used as a structural support material for metals but it's addition in small amount can modify the metal-based catalysts. For example oxidation of carbon monoxide can be carried out by using Au/TiO$_2$ at low temperature [20].

1.6.4. Application in photocatalysis

TiO_2 has been used for the photodegradation of organic compounds , for reduction of inorganic compounds and indoor odor removal as well [21].

1.6.5. Application as a white pigment

TiO_2 is white in color as it has high refractive index. Nano TiO_2 is opaque to light, chemically inert and doesn't fade in light. Because of these properties it is used in making paints which are used for buildings, industrial coatings and automobile finishes [22]. It is corrosion resistant and prevents photochemical degradation of light by absorbing UV light. It is also used as a pigment in optical devices as it has excellent optical transmittance.

1.7. Photocatalysis

Photocatalysis is composed of two words, "Photo" and "Catalysis". Photo means light and catalysis is a process where a substance modifies the rate of a chemical reaction without being consumed in that reaction and the substance used for modifying the rate of a chemical reaction by lowering the activation energy is called a catalyst.

Photocatalysis is a process where light is used to activate that particular substance which is used to modify the rate of a chemical reaction or to speed up a reaction and photocatalyst is that substance, which gets activated in the presence of light, generates electron-hole pair which modify the rate of chemical transformations [23].

One example of natural photocatalyst is chlorophyll of plants and nano-TiO_2 is man-made photocatalyst. The difference between these two is that when sunlight falls on chlorophyll, it utilizes that light to convert CO_2 and H_2O to glucose and oxygen. On the contrary, when sunlight falls on TiO_2 it causes the excitation of electrons to conduction band as a result a hole is created in the valence band. These charge carriers can be used to carry out the oxidation and reduction of organic contaminants converting them to CO_2 and H_2O.The difference between photocatalytic mechanism in TiO_2 and chlorophyll is shown in figure 1.3.
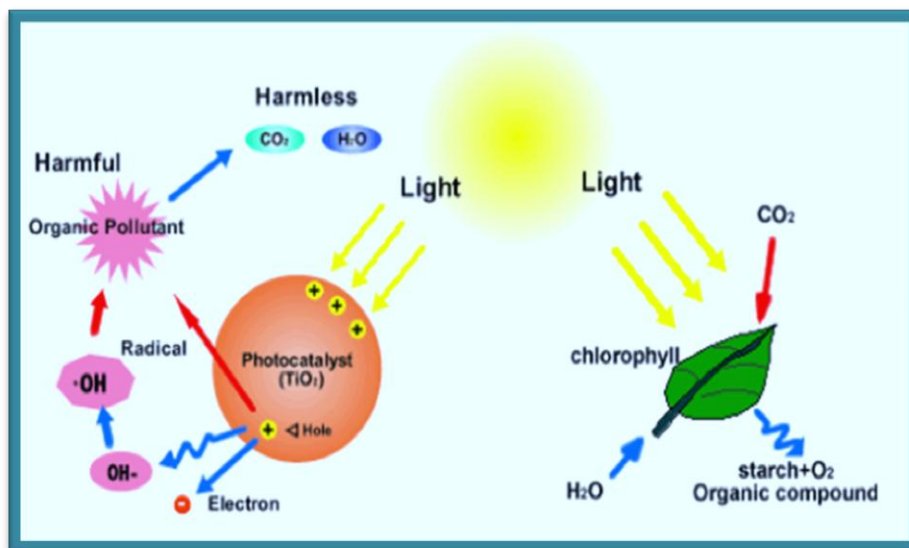
Figure 1.3 Difference between photocatalytic mechanism of TiO_2 and chlorophyll

1.7.1. Selection of a suitable semiconductor for photocatalysis

Several semiconductors are used for photocatalysis which include TiO_2, ZnO, CdS and WO_3 etc. An ideal photocatalyst should have following properties:

   i.   It should be stable under sunlight
   ii. It should be readily available
   iii. It should have low cost
   iv. It should be chemically inert
   v.   It should have the ability to adsorb the reactants

TiO_2 is the best semiconductor photocatalyst of all the semiconductors available, because of its ability to use solar light it can be used for the degradation of organic pollutants [24]. ZnO seems to be suitable alternative to TiO_2, as both have the same band gap, but it cannot be used for technical applications, as it degrades during repeated photocatalytic processes. CdS has a bandgap of 2.42 eV, which is lower than that of TiO_2, but it's photoactivity is decreased because of photo-corrosion resulting from self-oxidation [25].

1.8. TiO_2 as a photocatalyst

Fujishima and Honda discovered the photocatalysis of TiO_2 in their experiment in 1972. In their experiment, they used an electrochemical cell comprising of an inert cathode and an

electrode of TiO$_2$ rutile phase was used as anode. This cell was used for water splitting. After this experiment, extensive research was carried out to study the properties of TiO$_2$ as a photocatalyst and to use it for different applications including energy conversion and remediation of pollutants from environment [26]. After the discovery made by Frank and Bard in which they studied decomposition of cyanide by using TiO$_2$ in water, efforts were made to use it for environmental applications. Under UV light irradiation, it was found to be an effective photocatalytic disinfectant for microorganisms [27]. Among all the other semiconductors available this includes ZnO, CdS, WO$_3$ and MoS$_3$ etc. TiO$_2$ is the most efficient photocatalyst used especially for air and water treatment. The reason for it's for high efficiency is that it's oxidizing and reducing power is higher than other semiconductors. Along with that it is non-toxic, chemically inert and stable under sunlight and is corrosion resistant.

The band gap of anatase phase of TiO$_2$ is 3.3 eV due to which, it can only show it's photocatalytic activity under UV light. A band gap is an empty space between highest Fermi level of valence band and lowest Fermi level of conduction band. Electric conductivity of materials is related to band gap. Materials having no band gap are good conductors of electricity e.g. metals and materials possessing a wide band gap are bad conductors of electricity e.g. insulators. The band gap of semiconductor is intermediate between that of metals and insulators [28].

The photon of light when falls on TiO$_2$ it can excite electrons to conduction band and holes are created in valence band organic compounds can be oxidized and reduced by using these photogenerated electrons and holes. Mechanism of TiO$_2$ photocatalysis has been shown in figure 1.4.
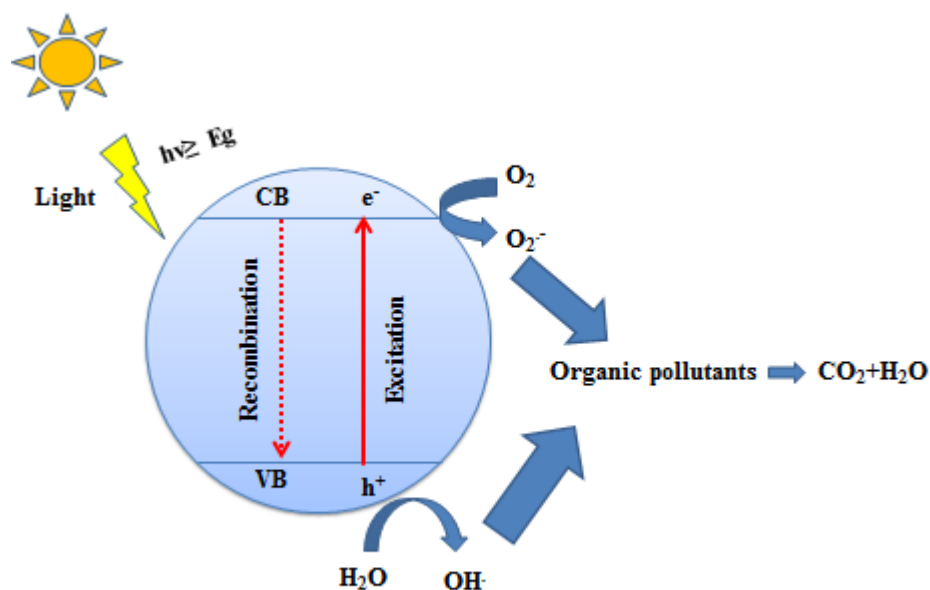
Figure 1.4 Mechanism of TiO_2 photocatalysis

Properties affecting the photocatalytic activity of TiO_2 are:

   i.   Surface area

  ii.   Crystallinity

 iii.   Crystallite size

 iv.   Crystal structure

Anatase has more open structure than rutile phase so it's photocatalytic activity is higher than rutile [29]. Research has been carried out for optimization of catalytic properties of TiO_2 by modifying titania or by using thin films of titania. Following are some of the modification strategies used for the modification of titania.

- Light sensitive dye is used for surface sensitization which causes the excitation of electrons in a semiconductor having wide band gap.
- Decreasing the size of TiO_2 nanoparticles increase the surface area which in turn increase the number of active sites leading to enhanced adsorption and degradation of pollutants.

- Coupling of TiO_2 semiconductor with another semiconductor having short band gap will also increase it's photocatalytic efficiency.
- Doping, in which metal or non-metal elements are introduced as impurities to TiO_2 semiconductor prevent the electron-hole recombination by trapping the electrons ejected from valence band, can also increase the efficiency of photocatalytic reactions [30].

1.9. Graphene

In 2004, a two-dimensional carbon material was reported by Geim and his coworkers which was named graphene [31]. Graphene is a single layer of graphite having thickness of one atom. In graphene 2D honey comb lattice is created by sp^2 hybridized carbon atoms making this structure favorable to be used as a precursor for other carbon materials. Graphene has unique optical, electrical and mechanical properties [32-34]. High mechanical strength of graphene is caused by σ-bond of carbon atoms with the neighbouring atoms. Half-filled orbital is formed by π-bonding of unused p orbitals with the neighbouring atoms. As a result highly conjugative structure is formed which is highly conductive in nature. Because of these high values of spring constant and Young's modulus, graphene is considered one of the strongest materials [32]. The electrical resistivity of graphene is less than the electrical resistivity of silver [33]. Graphene can absorb a significant part of white light because of its unique electronic structure making it suitable to be used for terahertz applications [33]. Heat conductivity of graphene is quite high. Embedding multiple layers of graphene onto silicon chip can increase the thermal characteristics to a greater extent [35].

Surface area of graphene is also quite high. According to theoretical calculations, surface area of graphene is 2630 $m^{2.}g^{-1}$. Because of high surface area and highly conjugated structure, graphene has the ability to adsorb other conjugated compounds forming π-π interactions. Work function of graphene is -4.42eV which is lower than that of TiO_2. As a result when TiO_2 is combined with graphene the recombination of electron-hole is prevented due to the trapping of photo-excited electron by conduction band of graphene.

1.10. Graphene oxide

The methods used for the production of graphene are expensive and complicated. Because of this reason some inexpensive methods have been developed for the synthesis and use of derivatives of graphene. Graphene oxide is a derivative of graphene possessing different functional groups including carbonyl, hydroxyl, carboxyl and epoxy. Because of these functional groups at edge and basal planes, sp^2 –bonded graphene network is converted to a combination of sp^2- and sp^3- hybridized carbon. Distortion in the conjugated π system is caused by these sp^3-defects lowering the strength and conductivity. The electronic, mechanical, and electrochemical properties of graphene oxide are strongly affected by these oxygen containing functional groups, therefore the properties of graphene oxide and graphene are quite different [36]. Electrical conductivity of graphene oxide is reduced because of oxygen containing functional groups, making it unfavorable to be used for electronic devices [37]. Hydrophilicity of GO sheets is increased because of these oxygen containing functional groups making it highly dispersible in different solvents which allow further modifications to be made to graphene oxide [38, 39].

Following four methods are used to synthesize graphene oxide:

1. Staudenmaier
2. Hofmann
3. Brodie
4. Hummers'

Many improvements and variations have been made these methods to get better results. A carbon/oxygen ratio of the graphene determines the effectiveness of an oxidation process.

1.11. Applications of graphene oxide

Because of transparency and high conductivity of graphene make it attractive to be used for different applications. The electronic structure and properties of graphene are quite unique. Because of zero band gap the charge mobility is quite high even at room temperature. Single layer graphene shows some unusual properties at room temperature e.g. quantum Hall effect and ambipolar characteristics making it suitable for electronics applications [40, 41]. Graphene is an efficient gas absorber due to its unique electronic

structure, high surface area and can be used for fabricating next-generation sensors [42]. Some fascinating applications of graphene are shown in fig. 1.5.

Electronics	Semiconductors	Gas absorbers
Sensors	Solar cells	Fuel cells
Optic devices		
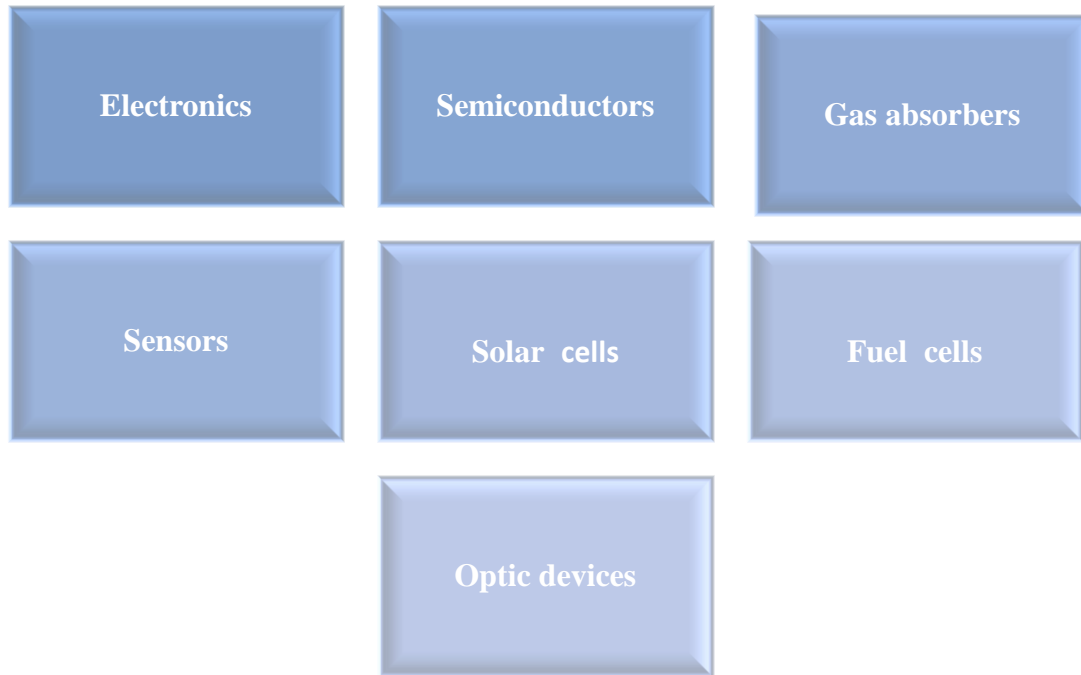
Figure 1.5 Applications of graphene

GO is non-conductive in nature because of introduction of oxygen containing functional groups on the GO basal plane. The sheet resistance value of GO is 10^{12} Ω sq^{-1} [43] . This insulating nature of graphene is because of sp^3 defects introduced in the structure. The carrier transportation is disrupted between sp^2 hybridized carbon clusters due to these defects making GO non-conductive in nature. However, GO can be made semiconductor by restoring sp^2 conjugated network of graphene. Various technologies are used for this reduction process which include chemical, thermal and electrochemical etc. The parameters of reduction process play an important role in determining the efficiency of reduction process. Heat treatment also increases the electrical conductivity by decomposing the oxygen functionalities which restore the sp^2 hybridization of carbon clusters. It was found in a study that sp^2 concentration and oxygen content in a fully reduced GO was 80% and ~8% respectively. This residual oxygen prevents the transport of charge carriers.

Nanoindentation in AFM was used to measure the intrinsic strength of graphene which was found to be 1.0 TPa and 130 GPa respectively [44]. AFM was also used to measure the

mechanical properties of GO sheets in a study and Yong's modulus of graphene oxide was found to be 207±23.4 GPa where the thicknesses of monolayer GO was 0.7 nm. As the 2D structure of graphene is altered due to the introduction of oxygen containing functional groups as a result the strength of GO is also lowered than graphene [45]. Introduction of functional groups brings changes in the molecular structure and binding energy of graphene making the graphene sheets unstable [46]. As a result the elastic properties of GO degrade. The introduction of sp^3 defects also lowers the thermal conductivity of graphene oxide.

Because of unique properties of graphene it can be used for the development of low molecular weight polymer composites which would be of high strength and can have applications in aerospace, automobile, food packaging and electronics etc.

1.12. Nanocomposites

A nanocomposite is a multiphase solid material in which one of the phases show dimensions in the nanometer range. Also in nanocomposites, the distance between different phases are also in the nanometer range. In nanocomposites different building blocks having dimensions in the nanometer range are used for the creation of new materials having improved flexibility and improved electrical, physical, optical and catalytic properties. Nanocomposites are attracting great attention as they have combined properties of individual components. The difference between the nanocomposite and conventional composite is the high surface to volume ratio of nanocomposites.

1.13. Graphene oxide (GO) based nanocomposites/nanocatalysts

Voitko et al. used graphene oxide for the decomposition of H_2O_2 and he found that the stability of GO in preserving it's photocatalytic activity over a large number of cycles is higher than any other carbonaceous material [47]. This stability of GO to retain is linked to the presence of oxygen containing functional groups at the basal planes and across the surface of sheets [47, 48] According to Lerf–Klinowski model, there are two distinct regions in the 2D structure of GO [48, 49]. First region consists of sp^2 hybridized carbon domains while the second region consists of oxygen containing functionalities including hydroxyl and epoxide groups at the basal plane and on the edges carbonyl and carboxyl

groups are present. These functional groups allow the stable dispersions to be formed due to easy dispersion of GO sheets in water and other polar solvents. The presence of ionizable carboxyl groups allow GO to act as ion-exchange resin allowing the exchange of ions with metal cations [50]. These properties allows the two-dimensional structure of GO to act as a support allowing the anchoring of metal or metal oxide nanoparticles on the edges and surface of GO [51]. The presence of sp^2 domains give rise to conducting pi-states along with that there exists a large band gap between sigma-states of sp^3 domains which are connected to oxygen containing functional groups [52]. These two factors make the electronic structure of GO heterogeneous. So by changing the carbon to oxygen ratio, the electronic properties of GO can be modified from insulating to semiconducting [53].

1.14. GO as catalyst support/co-catalyst

In heterogeneous catalysis, GO is used to disperse metal and metal oxide nanoparticles [54]. GO is preferred over other carbon supports in enhancing the efficiency of catalytic reactions because of following reasons.

i. The two-dimensional structure of graphene oxide allows easy dispersion of metal and metal oxide nanoparticles on its surface preventing their aggregation [55].

ii. The dispersibility of heterogeneous catalysts can be controlled by GO in aqueous solutions [56].

iii. The electronic structure of GO allows pi-pi interactions to be formed with organic compounds containing aromatic rings increasing their adsorptions for further oxidation/reduction [57].

iv. The light absorption range of the catalyst can be extended when combined with GO can prevent electron-hole recombination.

1.15. Nanocomposite of TiO_2-GO

Nanocrystalline titania is widely used as a photocatalyst because of its availability, non-toxicity and stability [36]. However, there are two factors limiting the use of TiO_2 in photocatalytic applications. These two factors are:

I. Rapid electron-hole recombination.

II.   Wide band gap because of which it is unable to absorb visible light from solar spectrum and only absorbs UV light which comprises only a small portion of solar spectrum.

To overcome these disadvantages, studies have focused on doping and co-doping of TiO_2 with metal and non-metal elements to extend the light absorption and to increase the photocatalytic efficiency of TiO_2 [36].

The recently discovered carbonaceous material graphene has attracted great attention because of its electronic structure and unique properties. Research has been carried out on the nanocomposite of TiO_2-GO which has shown increased photocatalytic performance because of reduced band gap and inhibited electron-hole recombination. These composites are highly stable and show excellent adsorption behavior [36].

1.16. Water contamination

The essence of water in our lives can be understood from the fact that no living being can survive on earth without water. Marine water covers the major part of water on earth which cannot be used for drinking purpose without processing. The only source of drinking water is fresh water which arises from ground water. Quality of water is very important in our life as physiological activities of biological cells depend mainly on water. Water comprises two third of our body weight and one cannot survive more than a few days without water. The human brain contains 95% water [58]. A reduction of 2% in our body's water supply can cause dehydration. Water is required by all the cells and organs making up our anatomy and physiology for their functioning [59].

Water contamination is the addition of harmful contaminants to drinking water to such extent that it cannot be used for drinking purpose by human beings and also is unfit to support the biotic communities such as fish [60]. Water pollution is not only harmful for organisms and plant living in these water bodies but also for natural biological communities. Water pollution has now become a global concern as it is increasing day by day and is causing numerous fatal diseases causing death of over 14,000 people on daily basis. Not only the industrial waste but also some natural phenomenon which includes algae blooms, storms and earth quakes are also affecting the quality of water. There are

different causes of water pollution. Addition of toxins to water make it unfit to sustain the living forms in it and becomes harmful for them.

1.16.1. Sources of water contamination

Water pollution is undesirable changes in the physical and chemical properties of water making it unfit for living organisms [60]. There are different sources of water contamination some of which have been discussed below.

Environment Protection Agency (EPA) published a report in 1990 which showed that more than 50% of the water pollution of water bodies is caused by the leaching of the chemical from landfills where they are used to increase crop production [61]. Another source of water contamination is municipal sources causing 12% of water contamination. Agricultural activities, industrials waste, mining are some of the sources of ground water contamination. The sources of water pollution are characterized as point source and nonpoint source. The direct emission of contaminants into water bodies is a point source for example the addition of industrial waste directly into the river is a point source of pollution. Whereas the addition of runoff of pollutants e.g. pesticide and fertilizers, to water bodies is a nonpoint source of pollution. Some major sources of water pollution are pesticides and dyes which have been discussed in detail below.

Pesticides

Pesticides are those chemicals which are used to increase the crop production by destroying the pests [62]. Although the pesticide should only target pests and not the other living organisms, but inappropriate application of these pesticide is affecting many living organisms including human beings [58]. The consumption of parathion contaminated wheat flour caused the death of about 100 people in India [63]. Pesticides cause several diseases by causing changes in body's immunity and reproductive system.

Pesticides Classification

1) Insecticides

An insecticide is a type of pesticide used to kill insects [64]. In the 20th century the use of pesticides has been increased to increase agricultural productivity. Insecticides can alter the ecosystem significantly and are toxic to human beings. Insecticides do not degrade immediately and take some time in their degradation. Some of the pesticides can persist in

the environment even for several years such as organochlorines. Persistence is the ability of pesticides to remain effective against pests for longer time. However, this long persistence of pesticides in the environment can also lead to water contamination under some conditions. Rainfall washes off these pesticides and when this rain water containing pesticides reaches water bodies it causes water contamination. Bioaccumulation of these pesticides in water bodies can pass them to other organisms including birds, mammals and human beings through the food chain [63].

2) Herbicides

Herbicides are type of pesticide used against herbs. Their small amount can cause the death of a highly sensitive plant. Herbicides can be selective or non-selective. Selective herbicides will harm only some plants whereas non-selective herbicides can be harmful for most forms of plants [58]. Some herbicides are water soluble and can easily enter into the water supplies through rainfall or irrigation water.

3) Fungicides

Fungicides are the type of pesticides used to harm fungi or fungal spores. Along with agriculture, fungicides are also used to treat fungal infections in different organisms. Fungicides are also used to control oomycetes as they follow the same mechanism as fungi do to affect the plants. Fungicides are of different types which include contact, translaminar and systemic fungicides. Contact fungicides only carry out the function of protection of those plant parts where they get sprayed. Translaminar fungicides redistribute themselves from upper surface of the leaf where they are sprayed to the lower surface. In systematic fungicides the redistribution takes place through xylem vessels to the upper parts of plant [61]. Fungicides are available in liquid and powder form. Sulfur is the most active ingredient present in fungicides which is present in lower concentration in liquid fungicides but in powdered fungicides 90% sulfur is present that's why powdered fungicides are highly toxic. Fungicides can enter into water supplies because of their improper application and disposal. Along with that they can also enter into water supplies through leaching and runoff from water supplies. Some fungicides can persist in the environment for a longer time and in this way can enter through soil and water causing their contamination [61].

Dyes

Dyes are complex aromatic molecules which are highly stable and therefore their degradation is quite difficult [65]. Commercially more than 100,000 dyes are available. Among one million tons dyes produced every year, 50% are textile dyes. Textile industry consumes tw0 third of total production of dyes. Among different types of dyes include

1. Natural dyes
2. Synthetic dyes
3. Food dyes

Among different dyes available commercially azo dyes comprise 60-70%. Azo dyes are used in different industries including textile, pharmaceutical and cosmetic industries [65]. Dyes are quite toxic as well so improper discharge of waste water containing dyes leads to serious skin and respiratory problems. Dyes are mainly used in textile industry and printing ink. Following are the effects of dyes in these two major industries.

Textile Industry*:* Till 19th century, only naturally produced dyes were used for textile industry.. The use of synthetic dyes started from the discovery of mauvine in 1856. Since then these synthetic dyes have been used extensively because of their several advantages which includes affordability, easy production and availability in different colors. Dyeing process in textile industry leads to the loss of 10-25% of textile dyes among them 2-20% are discharged in water causing water contamination [66]. This waste water is carcinogenic to different life forms because of the presence of harmful organic compounds including benzidine and naphthalene [67].

Printing Ink: Different heavy metals are used as pigments in printing industry which include titanium oxide, aluminum and brass. Leeching of these heavy metals into the water can cause serious health problems.

Following environmental and health hazards are caused by dyes:

1. When dyes enter into water they can absorb and reflect sunlight. This absorption of sunlight can easily inhibit photosynthetic activity of algae affecting the food chain
2. Mostly dyes are carcinogenic and are toxic to life [68].
3. Dye can cause cancer of kidney, urinary bladder and liver in the people working with them.
4. Textile dyes can cause different allergic reaction in eyes, skin diseases and respiratory problems.

5. The presence of small amount of dyes in water can affect transparency and quality of water to a greater extent which damages aquatic environment.

1.17. Characterization of the catalysts

Following techniques were used for the characterization of the catalysts.

1.17.1. Scanning electron microscope

Scanning electron microscope is one of the most important characterization techniques which is used to get information about topography, morphology and elemental composition. The resolving power of SEM is much higher than optical microscope and can achieve higher magnification. SEM was built by Manfred von Ardenne in 1930. In SEM analysis, surface images are obtained by scanning the surface of the sample with highly energetic beam of electrons. Highly energetic beam of electron interacts with the sample in two ways.

a. **Elastic collision:** Elastic collision causes a change in the path of electron beam without any loss of energy. Back Scattered Electrons (BSE) are generated as a result of this collision.

b. **Inelastic collision:** In inelastic collision, energy transfer from the beam of electron to sample occurs. Inelastic collision results in generation of Secondary Electrons (SE). In this study SEM images were taken by JEOL JSM-6460. For SEM analysis, the specimen should either be conductive or semi-conductive. The preparation technique involves the coating of the sample with several nanometer thick layer of a conductive material such as gold or platinum from a sputtering machine.

1.17.2. Energy dispersive spectroscopy (EDS)

EDS is analytical technique used to determine the elemental composition of a sample. SEM is equipped with EDS. EDS collects the data from SEM and that data is used to determine the elemental composition of the sample. Inelastic collision of electron beam with the specimen not only generates SE but it also generates characteristic X-rays and auger electrons due to the emission of inner shell electrons. These characteristic x-rays are detected by detector and spectrum is generated which shows different peaks corresponding to different elements.
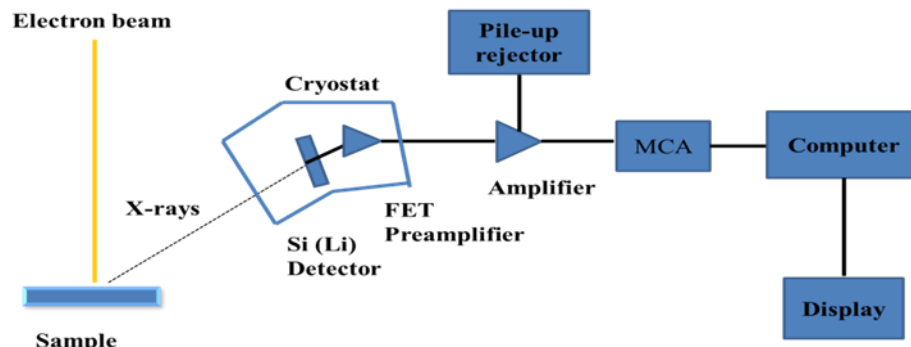
Figure 1.6 Schematic representation of EDS/EDX

1.17.3. X- ray diffraction (XRD)

XRD is an analytical technique which is versatile and non-destructive and used form the analysis of crystalline materials. This technique allows the study of structure of the material which includes crystallite size, d-spacing and arrangement of atoms. In XRD analysis, monochromatic x-rays interact with crystalline sample. X-ray beam is generated in a cathode ray tube by heating the filament. These x-rays are then passed through monochromator to get monochromatic x-rays which are then focused on the material to be analyzed. X-rays reflect back after being targeted on the material and are detected by the detector which are then processed and converted into signals. XRD data can be used to determine the crystallite size by using the Scherrer equation.

1.17.4. BET analysis for surface area measurement

Surface area of the catalysts was determined by BET analysis by using model NOVA 2200 e Quanta Chrome, USA. This equipment uses liquid nitrogen for adsorption. All the samples are degassed at 300°C for several hours and then adsorption of liquid nitrogen is carried out. A specific quantity of the sample is taken in the tube. After degassing, the samples are placed in a sample holder and inert atmosphere is created by passing the helium gas through the sample. In the end adsorption takes place through passage of nitrogen gas through the sample.

1.17.5. Fourier transform infrared spectroscopy

FTIR is a spectroscopic technique used for the identification of organic and inorganic compounds. This technique is non-destructive. The sample is exposed to infrared radiations. The interaction of these radiations with sample produces various stretching and bending vibrations at different frequencies which match with the frequencies of bonds present in the compound.

1.17.6. Diffuse reflectance spectroscopy (DRS)

DRS is an optical method which is commonly used to describe the electronic behavior present in the structure of materials in solid form. DRS and UV-Visible spectroscopy are closely related to each other. In both techniques, visible light is used to cause excitation of electron from valence band to conduction band. The difference between these two is that in UV-Visible spectroscopy, the relative change in transmittance of light is measured as it passes through sample, whereas in DRS the relative change in reflectance of light is measured. Kubelka-Munk transformation is used to manipulate the reflectance data into tauc plot.

1.18. Structure and objectives of thesis

This thesis describes the synthesis of TiO_2 nanoparticles by sol-gel method and graphene oxide by Hummer's method. Major task was to shift the absorption of TiO_2 from ultraviolet to visible region by doping it with nitrogen and cobalt. Nanocomposite of TiO_2-GO was synthesized to prevent electron-hole recombination.

First chapter summarizes the introduction about current research work. In second chapter, different papers related to this work have been discussed. Third chapter includes the methods for the synthesis of different catalysts. In chapter 4 results of current work along with degradation studies have been reported.

Following are the detailed objectives of current work:

- Synthesis of TiO_2 nanoparticles.
- Doping and co-doping of TiO_2 to shift it's absorption from UV to visible region.
- Characterization of prepared catalysts.

- Selection of best co-doped catalyst by carrying out the degradation of methyl orange.
- Preparation of Nanocomposite of graphene oxide with best co-doped catalyst in three different ratios.
- Photodegradation of methyl orange by using three different Nanocomposites and determining the best Nanocomposite.

2. Literature Review

2.1. Synthetic methods for TiO$_2$ nanostructures

2.1.1. Hydrothermal method

In hydrothermal method, autoclaves are used for the synthesis of nanomaterials under controlled temperature and pressure. This method is widely used in ceramic industry for the synthesis of nanoparticles. This method is also used for the synthesis of TiO$_2$ rods. Zhang et al. reported the synthesis of TiO$_2$ nanorods by hydrothermal method [21]. Treatment of dilute solution of TiCl$_4$ at 333-423 ∘K for 12 hours in the presence of acid resulted in the formation of nanorods. This method is also to synthesize nanotubes of TiO$_2$ [21].

2.1.2. Solvothermal method

In this method the solvent used is non-aqueous. As the organic solvents used in this methods can have high boiling points so the temperature can also be quite high. This method can be used to control different properties of nanoparticles i.e. Particle size, crystallinity and shape distribution [21].

2.1.3. Sol-gel method

In sol-gel process metal alkoxides are used as precursors. A colloidal suspension called sol is formed from the Hydrolysis and polymerization of metal alkoxides. This sol is converted to a solid gel after evaporation of the solvent. Nanoparticles of TiO$_2$ are synthesized by this method from the hydrolysis of titanium precursors. This hydrolysis step is catalyzed by acid followed by condensation. Polycondensation of alkoxides precursors in the presence of tetramethyl ammonium hydroxide results in the formation of highly crystalline TiO$_2$ nanoparticles [69].

2.1.4. Chemical vapor deposition method

The condensation of any material from vapor state to solid state is called vapor deposition. By using this method coatings are formed on different substrates to modify their properties. These properties include mechanical, electrical, thermal and corrosion resistance etc. Djerdja et al. used CVD method for the deposition of nanocrystalline films of TiO_2 on different substrates. He concluded that nature of substrate plays a very important role in determining the size and distribution of nanograins in TiO_2 films [70].

2.1.5. Sonochemical method

Many nanostructured materials are synthesized by ultrasonication. TiO_2 nanoparticles are prepared by dissolving 0.5 g TiO_2 pellets in 30 ml NaOH solution. This solution is stirred for 2 h at room temperature. The yellowish solution obtained is ultrasonicated for 2 h. The precipitates formed are then centrifuged and washed with water and then dried at 60∘C. Zhu et al. synthesized TiO_2 nanotubes by sonochemical method [69].

2.2. Comparison of photocatalytic activity of different phases of TiO_2

Anatase, rutile and brookite are three different phases of TiO_2. All of these phases have same structure which is octahedral but the arrangement of atoms in these structures is different. Anatase and rutile have tetragonal structure whereas the structure of brookite is rhombohedral [71]. Rutile phase of TiO_2 is thermodynamically stable whereas other two phases are metastable. Extensive research has been carried out on anatase phase as it shows higher photocatalytic activity compared to other two phases. TiO_2 undergoes transformation of phase from anatase to rutile above 600 ºC. Anatase phase of TiO_2 has a band gap of 3.2 eV which is larger than that of rutile. As there is inverse relation between the magnitude of band gap and recombination probability of electron-hole pairs so it means electron-hole pair recombination takes place slowly in anatase phase compared to rutile resulting in higher photocatalytic activity of anatase [72].

2.3. Factors affecting the photoactivity of TiO_2 nanoparticles

Following are the factors which affect the properties of TiO_2 nanoparticles.

2.3.1. Influence of precursor concentration

High concentration of TTIP precursor results in generation of large concentration of TiO_2 nuclei which in turn cause coagulation and sintering resulting in increased particle size. The transformation of phase from anatase to rutile is also increased with increase in precursos concentration [73].

2.3.2. Influence of water content

Hydrolysis reaction.is affected greatly by amount of water. Xiaobo et al. reported that low water content and excess amount of precursors results in low hydrolysis rate. Less amount of water causes incomplete hydrolysis of alkoxides. Barringer and his coworkers deduced the ratio of water to alkoxides from the equation $R = [H_2O]/ [TEOT]$ and it was found that this ratio should be greater than 2.5 for appropriate particle size. The largest ratio which was reported was 7 which resulted in particle size of 300 nm [74].

2.3.3. Influence of pH

The pH plays a very important role in controlling the size and shape of nanoparticles [75]. Increase in pH of the sol results in increased grain size [76]. Increased hydrogen ion concentration decreases the nucleation rate and particles grow rapidly resulting in formation of large grains. As a result new nucleus gets sufficient time to grow and results in formation of large TiO_2 particles through aggregation. pH also determines stability of the sol.

2.3.4. Influence of temperature

In sol-gel process the most critical parameter which controls the properties of nanoparticles is temperature. The effect of temperature on particle size was studied by Vorkapic and his coworkers by varying the temperature from 0-50 °C [77]. They found out that low temperature results in the formation of large particles. Particle size decreases with increase in temperature. Optimum temperature range for sol-gel process is 25-50 °C. Thermal energy of the colloid increases at high temperature resulting in decrease in viscosity and dielectric constant of the solvent and in this way electrostatic barrier against aggregation is lowered and formation of larger particles occurs [78].

2.3.5. Influence of precursor type

The effect of different alkoxy precursors on particle size was investigated by Vorkapic and his coworkers and they found out that increase in length of alkoxy group decreases the particle size because of decrease in reactivity and hydrolysis rate [79]. According to their results the decrease in particle size was of the following order. Ethoxide > propoxide ≥isopropoxide > butoxide.

2.3.6. Influence of type of solvent and concentration

In general, after the formation of nuclei particles growth occurs by aggregation or molecular addition. This particle growth is affected greatly by the kind of solvent used because particles interact differently in different solvents. Particle size increases with increase in concentration and molecular weight of the alcohol and without alcohol smallest sized particles are formed [79]. The reason is that the dielectric constant of the solvent and stability decreases with increase in amount and molecular weight of alcohol as a result rate of re-aggregation is increased and large size particles are formed.

Xu et al investigated that content of anatase increase and particle size decreases with increase in chain of the solvent (which is used for preparing nanoparticles) which in turn increases the photocatalytic activity of TiO_2 nanoparticles [80]. They found that by using methanol anatase phase content was 68% which was increased to 91% by using 2-propanol and particle size also decreases from 11.6 nm to 10.5 nm. In a sol-gel process increased concentration of alcohol decreases the hydrolysis rate as a result the content of amorphous TiO_2 in the sol also increases.

2.4. Modifications of TiO_2 nanomaterials

Along with applications in photocatalysis, TiO_2 has applications in biomedicine and are also used in sensors as well. Physiochemical characteristics affect the performance of TiO_2 in these applications to a greater extent. These physiochemical properties include surface area, crystallinity, crystallite structure and quantum efficiency etc. [25].

For example, to obtain higher photon capture efficiency in solar applications narrow band gap of TiO_2 is required. TiO_2 only absorbs the UV radiations and not the visible radiations.

Because of this reason it cannot use solar light effectively which contains 95 % visible light [81]. Research has been done for the modification of the properties of TiO_2 by shifting it's response from ultraviolet to visible region. These modifications can be divided into two groups.

    i.   Bulk modification

   ii.   Surface modification

Bulk modification

Bulk modification involves the doping of foreign elements to modify the performance of TiO_2 [82]. There are two approaches of bulk modification. First approach involves the addition of Zr, Al or Si which increase the thermal stability and surface area of TiO_2 nanomaterials. In second approach some metallic and non-metallic elements are added to shift the absorbance from UV to Visible region. These elements include Fe, Cr, V, Mn, Co C, N, S etc. Sometimes, co-doping of metallic and non-metallic elements is carried out to achieve desirable properties. Wang et.al used nitrogen doped TiO_2 for the oxidation of organic compounds. He reported that the addition of ZrO_2 has enhanced the photocatalytic activity greatly by increasing the surface area and preventing grain growth [83].

Surface modification

Colored organic and inorganic compounds are used for sensitizing TiO_2 which in turn enhance the optical absorbance of TiO_2 in the visible region. Surface modification of TiO_2 with other semiconductors is carried out to prevent electron-hole recombination [84].

2.4.1. Bulk modification of TiO_2 nanomaterial

Numerous studies have focused on modification of TiO_2 for the shifting of band gap from ultraviolet to visible region which in turn allows for efficient utilization of solar energy [85]. Doping of TiO_2 with different metals and non-metals reduces the band gap and enables TiO_2 to absorb in the visible region. Doping with transition metals also prevents electron-hole recombination as they act as electron-hole trap site. These transition metals include Fe, Mn, Cr and Co etc. [85, 86]. Doping with cobalt has been extensively studied as it has unique electronic structure and size which resembles with that of TiO_2.

TiO_2 is also modified with anions to shift its absorption over a broad range. These anions include C, F, N and S. Asahi et al. reported that among all anions, doping with N has the most pronounced effect in narrowing of the band gap [87].

Studies have also shown that crystallinity, surface area and thermal stability also affect the activity of TiO_2. These properties can be modified with synthesis method, heat treatment and type and amount of doping [88]. Modification in textural properties can also increase photocatalytic performance of TiO_2. According to studies surface area of mesoporous TiO_2 is quite large and also has uniform pore structure therefore they show high catalytic performance. Research has shown that incorporation of some metals into the framework of silica stabilizes its structure. Wang et al. used this approach for doping of TiO_2 with Fe by hydrothermal process and the resulting material had well-ordered mesoporous structure [89]. Some other dopants are also used to increase thermal stability and surface area. These dopants include Al, Si and Zr but the extent to which these dopants can be effective depends strongly on the synthesis method and composition [90]. In solar energy applications, Zr has a pronounced effect in increasing the thermal stability and activity of TiO_2. Research has shown that TiO_2-ZrO_2 shows higher activity than pure TiO_2 and pure ZrO_2 because of enhancement in surface area [91].

Noble-metal doped TiO_2 nanomaterials

Nobel metals for example Au, Pd, Pt and Rh are found to be quite effective for increasing the photocatalytic performance of TiO_2 by lowering the band gap. Bamwenda et al. doped TiO_2 with Au and Pt and investigated their effect on the photocatalytic performance of TiO_2. Seery et al. doped TiO_2 with silver for the reduction of band gap [92].

Different methods have been used for the synthesis of noble metal doped TiO_2 which includes sol-gel, photo-deposition method, impregnation method and hydrothermal process. Photocatalytic performance of TiO_2 doped with noble metals depends on the method used for synthesis and the type of noble metal used. Pt and Au are found to be most effective in increasing the activity of TiO_2 [92].

Transition metal doping

Transition metal doping of TiO_2 results in significant reduction in band gap and improves photocatalytic performance of TiO_2. Due to Transition metal doping, different impurity levels are created in the band gap as a result significant reduction of band gap takes place

and hence absorption shifts in the visible region. Along with that electron-hole recombination is also prevented because of the transfer of electrons from conduction band of TiO_2 to transition metal ions. Choi et al investigated the photocatalytic performance of TiO_2.by doping with 21 different transition metals Doping with these transition metals resulted in visible light absorption. Choi found that among different transition metals Mo, V, Rh, Re and Fe were the most effective in increasing the photocatalytic performance of TiO_2 [93].

Hashimoto et al. doped TiO_2 with Fe (III) and Cu (II) and used it for the degradation of 2-propanol in the presence of visible light. In this case, the transfer of charge from valence band holes to the dopants resulted in visible light activation. Wu et al. studied acetic acid degradation by Cr, Co, Ni and Fe doped TiO_2. They concluded that these ions are quite effective in increasing the photocatalytic activity as they prevent electron-hole recombination [93]. Amadelli et al. used impregnation method for the synthesis of cobalt doped TiO_2 and they found out that cobalt doped TiO_2 shows higher photocatalytic activity This enhancement in photocatalytic activity depends on amount of dopant added and synthesis method [94].

Non-metal doping

Anion doping is a new method used to increase photocatalytic activity of TiO_2. Different anions for example N, F, S and C cause improved absorption of visible light. Asahi et al. doped TiO_2 with different anions and also determined their doping content. He found out that nitrogen doped TiO_2 was the efficient catalyst among all [95]. Different physical and chemical methods are used for the synthesis of N-doped TiO_2. In sol-gel process different precursors which are used for nitrogen doping are urea, diethanol amine, triethanol amine and 1, 3- diaminopropane. Studies have shown that visible light absorption is caused by lattice nitrogen whereas the nitrogen present at the surface results in band gap narrowing.

Kisch and his coworkers used carbon modified TiO_2 for photocatalytic applications [96]. Carbon doped TiO_2 showed improved photocatalytic activity compared to undoped TiO_2 because of significant reduction in band gap [97]. Depending on the preparation method carbon doping can be interstitial or substituional. Umebayashi et al. synthesized anionic S-doped TiO_2 by thermal oxidation of TiS_2 [98] and Ohno et al. synthesized cationic Sulphur doped TiO_2 by using TTIP and thiourea [99]. These S- doped materials were used for the

photocatalytic degradation of methylene blue and 2- propanol and have shown improved photocatalytic activity. F- doping has also been found to increase the photocatalytic activity of TiO_2. Yu et al. reported that F- doping causes reduction of Ti^{4+} to Ti^{3+} which in turn reduces the band gap [100].

Metal non-metal co-doping

Metal non-metal co-doping is found to be quite effective in increasing the photocatalytic activity of TiO_2 under visible light. Different co-doped catalysts have been synthesized and it has been found that co-doped TiO_2 shows higher photocatalytic activity than mono-doped TiO_2. For example Nb and nitrogen co-doped TiO_2 is 7 times more efficient than undoped TiO_2 [101]. N- Ga co-doped TiO_2 has been found to be highly efficient in water splitting [102]. Li et al. synthesized C and Mo co-doped TiO_2 by hydrothermal method [103]. This co-doping resulted in significant reduction in band gap because of adsorption of carbon on the surface and presence of Mo^{6+} in the lattice. This co-doped catalyst also prevents electron-hole recombination. Thind et al. developed a solution combustion method for the synthesis of N, W co-doped TiO_2 which was found to be highly efficient in the degradation of Rhodamine-B [104].

In transition metal- nonmetal co-doping, electron hole recombination is prevented due to charge transfer by metals in non-metal doped TiO_2. As co-doping combines the feature of both dopants so it increases the photocatalytic activity of TiO_2. Dola et al. compared the photocatalytic activity of Fe, N co-doped TiO_2 with N doped TiO_2 and Fe doped TiO_2 and he found that the photocatalytic activity of Fe, N co-doped TiO_2 is higher than other two catalysts under visible light [105]. Liu et al. reported that Co, N co-doped TiO_2 extends the absorption into the visible region by narrowing the band gap [106]. Zhang et al. reported that Ni, N co-doping prevents electron- hole recombination [107]. Jia wang et al. synthesized (Ni, Co, Fe) - N co-doped TiO_2 and compared their photocatalytic performance and they concluded that N, Co co-doped TiO_2 increases the photocatalytic activity by 10 times than undoped TiO_2 [108].

2.4.2. Surface modification of TiO_2 nanomaterials

Following methods are used for the surface modification of TiO_2.

Dye-sensitization

Dye-sensitization is used widely in photocatalytic reactions for effective utilization of solar light. As dyes can absorb visible light so when they are irradiated with visible light electrons get excited from valence band to conduction band which are then transferred to the conduction band of TiO_2 [109]. This electron transfer increases photocatalytic activity of TiO_2. One the main issues of dye-sensitization is dye degradation itself. To overcome this limitation sacrificial agents are used which cause dye regeneration. The main advantages of dye-sensitization is fast transfer of electrons to the conduction band of semiconductor while the backward reaction takes place slowly [110].

Heterojunction semiconductors

Semiconductors having different band gap values are also coupled together to improve conduction band more negative than the other. In semiconductor heterojunction when light falls on one of the semiconductor having more negative conduction band electron get excited from valence band to conduction band which are then transferred to the conduction band of less negative semiconductor and in this way electron-hole recombination is prevented. Research has been carried out on the coupling of TiO_2 with CdS and SnO_2 which were used for splitting of water and other photocatalytic applications [110]. Doong et al. coupled TiO_2 with CdS and used it for the photodegradation of 2- chlorophenol [111]. In this case, as CdS have more negative conduction band so the transfer of electron occurs from conduction band of CdS to that of TiO_2. Highest photocatalytic activity was shown by nanocomposite.

Keller and Garin studied the photocatalytic activities of TiO_2–WO_3 and TiO_2–SiC composite. In case of TiO_2–SiC, SiC has more negative conduction band so transfer of electron occurs from the conduction band of SiC to the conduction band of TiO_2. Whereas in case of TiO_2- WO_3 composite, the transfer of electron takes place to the conduction and of WO_3 from that of TiO_2. These composites have shown higher photocatalytic activity in the photodegradation of methyl ethyl ketone because of improved electron- hole separation [112].

2.5. Nanocomposites of TiO_2/graphene oxide

Graphene oxides contain highly reactive oxygen containing functional groups and there are used in many applications. Graphite is used for the synthesis of graphene and graphene

oxide. Graphene has limited application as it has lower dispersibility in water and reduced surface area. Therefore research has been carried out on coupling of graphene oxide with some other materials having good dispersibility in water. Graphene oxide is formed through chemical oxidation of graphene. Controlled oxidation tunes the mechanical and electronic properties of graphene oxide. Various functional groups on graphene oxide can be chemically modified for the generation of materials having amazing properties [113].

Brodie synthesized graphene oxide for the first time in 1859 by oxidizing graphite with $KClO_3$ in the presence of nitric acid. Later in 1898, this method was further modified by Staudenmaier by replacing nitric acid with concentrated sulphuric acid and also the $KClO_3$ was added slowly in several aliquots. This method was further improved by Hummer and Offeman. They used $KMnO_4$, $NaNO_3$ and H_2SO_4 for the oxidation of graphite. This method has now been further modified [113].

Extensive research has been carried out on the fabrication of graphene oxide based nano-composites. Nano-composites of graphene oxide with TiO_2, ZnO and WO_3 can increase their photocatalytic activity by preventing electron-hole recombination. Maruthamani et al. synthesized the nano-composite of rGO/TiO_2 and used it for the degradation of Rhodamine B. He also studied on the effects of initial dye concentration, rGO content initial concentration of dye, pH concentration of dye on the photocatalytic activity. They concluded that increasing the rGO content in the composite cause attachment of more TiO_2 particles onto the rGO sheet and thus increase photodegradation process. Degradation of Rhodamine increases with increase in catalyst concentration up to 1.5 g L^{-1} due to increase in number of active sites resulting in enhanced adsorption of dye onto the catalyst surface. The photodegradation activity of the catalyst decreases with further increase in concentration of the catalyst due to increased agglomeration of catalyst particles and increased turbidity of the suspension making light penetration more difficult [114].

Nanocomposites of GO/TiO_2 are widely studied. TiO_2 is the most widely used semiconductor because of its stability, non- toxicity and low cost. But of the major drawback to limit the photocatalytic activity of TiO_2 is rapid electron-hole recombination [115]. Preparing nano- composite of GO/TiO_2 overcomes this limitation due to transfer of photo-excited electron from conduction band of TiO_2 to that of graphene oxide. Gao et al. used GO/TiO_2 for modification of surface of polysulfone based membrane used for water

purification. Four different morphologies of TiO_2 were coupled with graphene oxide. All of these different catalyst showed different photocatalytic performance [116].

Hemraj M. Yadav used two step methods for the synthesis of TiO_2-GO nanocomposite. Sol-gel method was used for the synthesis of TiO_2 nanoparticles. Solvothermal method was used for preparing the nanocomposite. This composite was used for the photocatalytic degradation of benzene gas under ultraviolet light. Results showed photocatalytic activity of composite was 3 times higher than that of pure TiO_2 [117].

Vaclav Stengll et al. used liquid phase deposition method for deposition of TiO_2 on graphene oxide sheets. This composite was used for the photodegradation of n-butane. The surface area of the composite increases with increase in amount of graphene oxide. Along with that because of $\pi-\pi$ conjugations between butane molecule and aromatic rings of graphene oxide leads to efficient adsorption of the n-butane onto the surface of the composite. Graphene oxide along with preventing electron-hole recombination also ensures efficient adsorption of n-butane leading to enhanced photodecomposition [118].

3. Materials and Methods

3.0. Introduction

This study was aimed to synthesize TiO_2 nanoparticles, co-doping of these TiO_2 nanoparticles with nitrogen and cobalt and preparation of nanocomposites of one the co-doped nanoparticles with graphene oxide. Sol-gel method was used to synthesize un-doped and co-doped TiO_2 nanoparticles as it is the most simplest of all the methods available. Furthermore, particle size, morphology and distribution can easily be controlled by using this method.

Graphene oxide was synthesized by using Hummers' method which is a safe and fast method and by using this method a high C/O ratio is maintained. Along with synthesis methods, different characterization techniques used for the synthesized nano-materials have also been outlined in this chapter.

3.1. Synthesis of TiO_2 nanoparticles by sol-gel method

3.1.1. Chemical reagents/materials

The following chemical reagents were used in this study: titanium (IV) tetraisopropoxide (TTIP), 2-propanol, nitric acid, urea, cobalt (II) nitrates hexahydrate, nitric acid was supplied by Merck and deionized water was also used.

3.1.2. Synthesis of TiO_2 nanoparticles

Titanium (IV) tetraisopropoxide (TTIP) was the main starting material and no further purification was made to it. TTIP (5 mL) and 2-propanol (6 mL) were mixed together to form solution **A.** A few drops of nitric acid were added to water (85 mL) to adjust it's pH to 2 and it was designated as solution **B**. Dropwise addition of Solution A into solution B was carried out under vigorous stirring. The mixture was stirred overnight at room temperature. Dried powder was obtained by evaporating the solvent in rotary evaporator. This powder was calcined at 450 °C for 4 hours in the furnace and then grinded for 1 hour .

The obtained nanoparticles were characterized by XRD, SEM, BET, FTIR, EDX and UV-VIS spectroscopy.
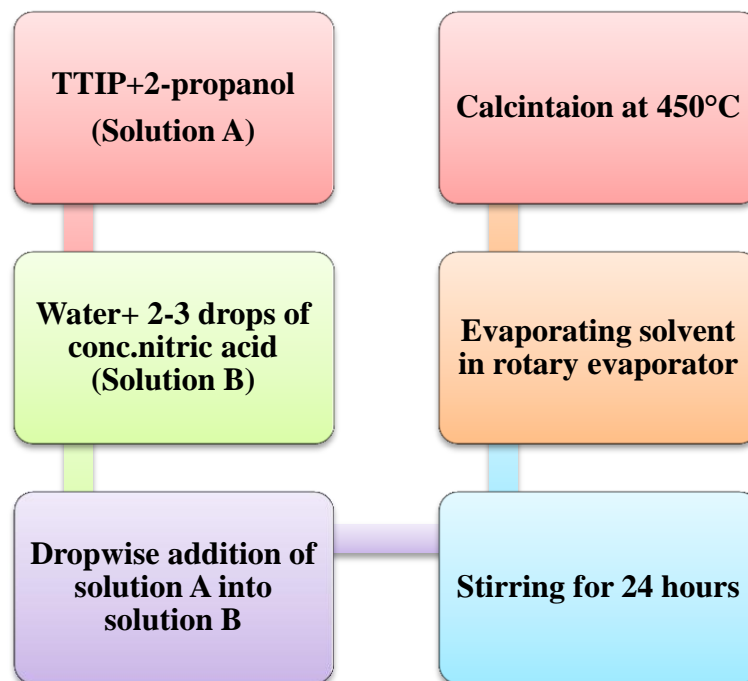
Figure 3.1 Flow diagram of synthesis of TiO$_2$ nanoparticles by sol-gel

3.1.3. Synthesis of nitrogen doped TiO$_2$ nanoparticles

Nitrogen doping of TiO$_2$ was carried out by using the same method as described in section 3.1.2. 3 g urea was added to solution B under vigorous stirring. Then solution A was added to solution B dropwise. This mixture was left for stirring overnight and then solvent was evaporated by using rotary evaporator. Dried powder obtained was calcined at 450 °C for 4 hours in the furnace. Obtained powder was yellow in color and it was grinded by using agate mortar and pestle for 1 hour. . The obtained nanoparticles were characterized by XRD, SEM, FTIR, BET, EDX and UV-VIS spectroscopy.

3.1.4. Co-doping of TiO$_2$ nanoparticles with nitrogen and cobalt

Co-doping of TiO$_2$ with nitrogen and cobalt was carried out by the same method as described in section 3.1.2. 3g urea was added to solution **B** under vigorous stirring and different amounts of cobalt nitrate i.e. 10mg, 50mg, 100mg, 500mg and 1g were also

added to solution **B.** Then solution **A** was added drop-wise to solution **B.** This mixture was stirred overnight and after that solvent was evaporated by using rotary evaporator. Dried powders were calcined at 450°C for 4 hours in the furnace. Obtained powder was of green color with the color getting darker with increasing dopant concentration. Powder was grinded for 1 hour using agate mortar and pestle. The obtained nanoparticles were characterized by XRD, SEM, EDX and UV-VIS spectroscopy.

Table 3.1 Indices of samples and experimental details

Sample ID	Sample Composition	TTIP: Urea (Mass ratio)	TTIP: $Co(NO_3)_2.6H_2O$ (Mass ratio)	Calcination Temp.
TiO$_2$	Titanium dioxide nanoparticles	-	-	450 °C
N-TiO$_2$	Nitrogen doped titania nanoparticles	1:3	-	450 °C
CoN-TiO$_2$-1	Co and N doped titania	1:3	1:0.0032	450 °C
CoN-TiO$_2$-2	Co and N doped titania	1:3	1:0.016	450 °C
CoN-TiO$_2$-3	Co and N doped titania	1:3	1:0.032	450 °C
CoN-TiO2-4	Co and N doped titania	1:3	1:0.16	450 °C
CoN-TiO$_2$-5	Co and N doped titania	1:3	1:0.32	450 °C

3.2. Synthesis of graphene Oxide

3.2.1. Chemical reagents/materials

Following chemical reagents were used for the synthesis of graphene oxide: Graphite powder, sodium nitrate, potassium permanganate, sulphuric acid, hydrogen peroxide and deionized water.

3.2.2. Synthesis of graphene oxide

Graphene oxide was synthesized by using Hummers' method. In this method graphite powder (1 g), conc.H_2SO_4 (23 mL) and sodium nitrate (0.5 g) were added together in a 500 ml flask. This flask was kept in an ice bath with continuous stirring. When the temperature approaches 0°C, potassium permanganate (3 g) was added to this suspension very slowly with continuous stirring. As addition of potassium permanganate is an exothermic reaction so the rate of addition of potassium permanganate to the suspension was carefully controlled so that the temperature doesn't go above 15°C. This mixture was kept for stirring for 1 hour at 30°C. After that deionized water (150 mL) was added to it very slowly and color was changed to brown. Mixture was again kept for stirring for 2 hours. After 2 hours 30% H_2O_2 aq. solution was added resulting in change in color from brown to yellow, the mixture was allowed to stir for 15 minutes and then sonicated for 1 hour. The mixture was centrifuged at 4000 rpm for 40 minutes to obtain graphene oxide and the resulting graphene oxide was washed with 10 % HCl then with deionized (DI) water and in the end it was dried at 60°C under vacuum. The obtained nanomaterial was characterized by XRD, SEM, EDX and UV-VIS spectroscopy.

3.3. Synthesis of RGO/Co, N-TiO$_2$ nanocomposites

3.3.1. Chemical reagents/materials

As prepared nitrogen and cobalt doped TiO$_2$ nanoparticles and graphene oxide.

3.3.2. Procedure

Graphene oxide was ultrasonically dispersed in 80 ml of water. After that certain amount of co-doped TiO$_2$ nanoparticles were added to it and the mixture was stirred for almost one hour. Then the mixture was transferred to an autoclave of 100 ml capacity and it was held in electric oven at 120°C for 4 hours. After that the product obtained was washed with deionized water several times and then the slurry obtained was dried in vacuum oven at 60 °C.

4. Results and Discussion

In this chapter, the characterization and structural properties of as prepared undoped and co-doped TiO_2 nanoparticles and nanocomposite of N, Co co-doped TiO_2 with reduced graphene oxide has been explained. The degradation studies of methyl orange have also been included in this chapter.

4.1. Results of structural and optical properties of the catalysts

Samples were analyzed by different techniques to study their structural and optical properties.

Results of these analyses are explained below;

4.1.1. Scanning electron microscopy (SEM) results

The morphology and particle size of as prepared catalysts was examined by SEM analysis. SEM images were taken by JEOL JSM-6460 which is also equipped with energy dispersive X-ray spectroscopy (EDS) to allow compositional analysis of samples to carry out. SEM images show that the nanoparticles have average particle size below 40 nm. These nanoparticles are spherical and are evenly distributed.
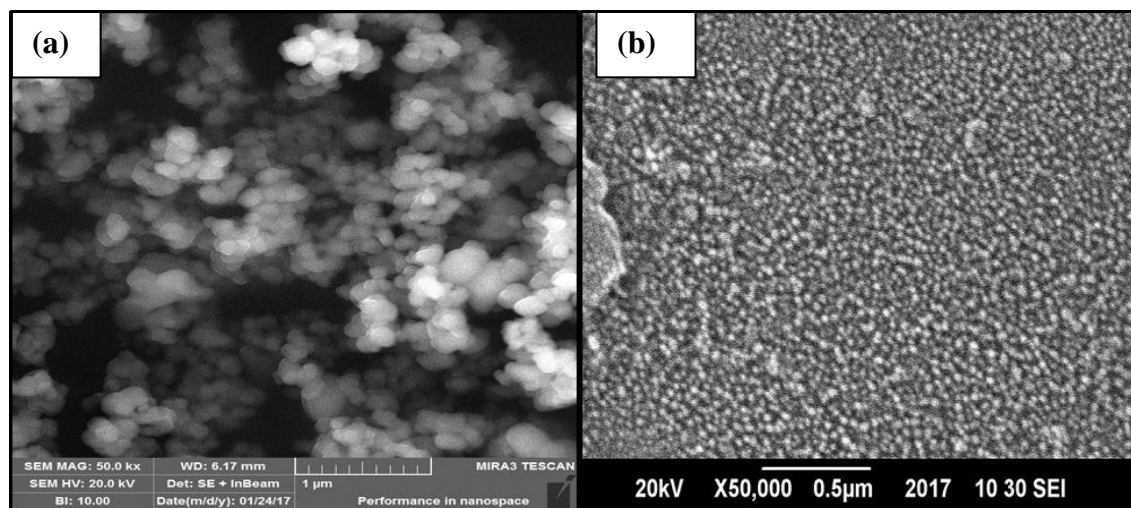

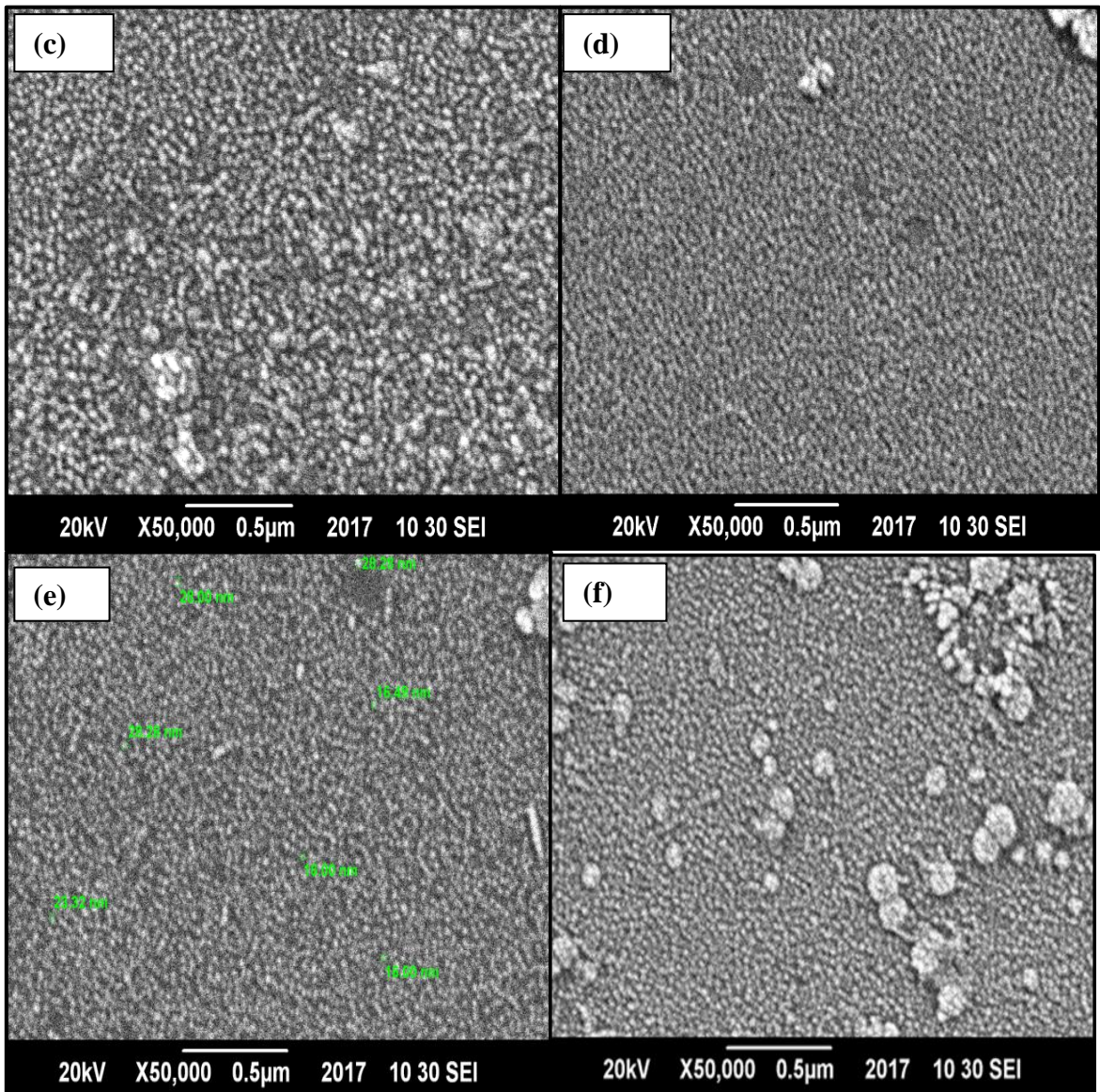**Figure 4.1** SEM analysis of (a) TiO_2 (b) N-TiO_2

Figure 4.2 SEM analysis of (c) CoN-TiO$_2$-1 (d) CoN-TiO$_2$-2 (e) CoN-TiO$_2$-3 (f) CoN-TiO$_2$-4
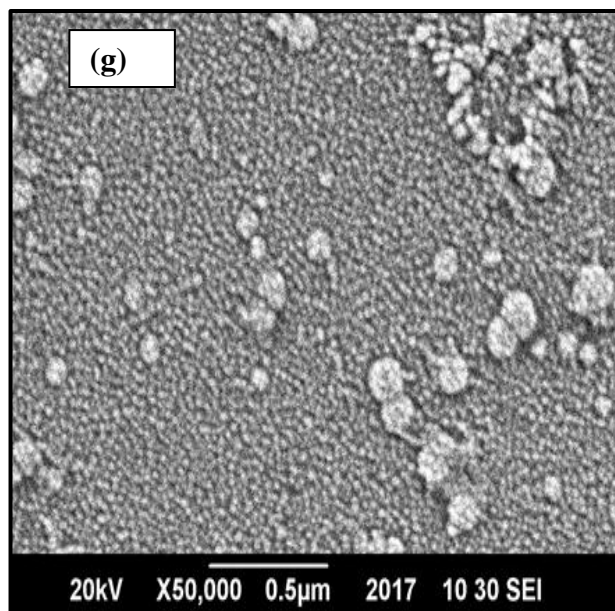
Figure 4.3 SEM analysis of (g) CoN-TiO$_2$-5

Figures from 4.1 to 4.3 show the SEM images of undoped TiO$_2$, N-TiO$_2$ and co-doped TiO$_2$ which were prepared by sol-gel method and calcined at 450 °C. There is no change in the morphology of doped and co-doped TiO$_2$ nanoparticles after adding with nitrogen and cobalt ions. In case of doped catalysts the average particle size is in the range of 20-40 nm. Whereas, in case of undoped TiO$_2$ nanoparticles the particle size is ~60 nm .The spherical morphology of these nanoparticles not only designs the surface properties and surface area but also tunes the electronic structure i.e. improves the photocatalytic activity by making visible light spectrum more active [119].

Figure 4.4 shows the SEM images of graphene oxide. These SEM images show that graphene oxide contains randomly aggregated, thin crumpled sheets having thickness in the range of micrometer. The thickness of these sheets can be in the nanometer range depending on the number of stacked sheets.
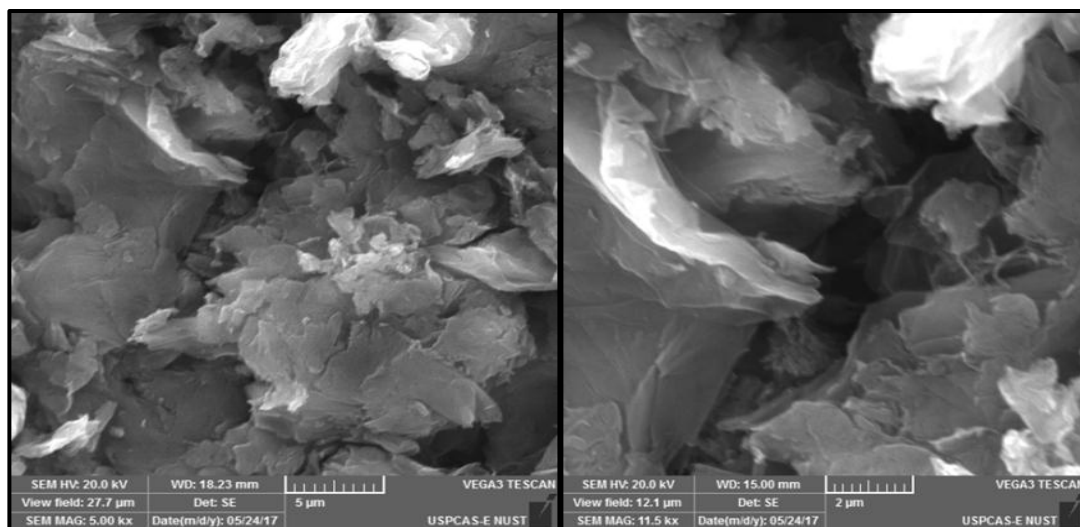
Figure 4.4 SEM analysis of graphene oxide sheets

Figure 4.5, 4.6 and 4.7 show SEM images of nanocomposites. In these SEM images we can see co-doped TiO_2 nanoparticles which are decorated on the surface of reduced graphene oxide. This interaction between RGO sheets and co-doped TiO_2 nanoparticles can promote charge transfer between them and can also increase adsorption of methyl orange due to the excellent electron conductivity of these graphene sheets.
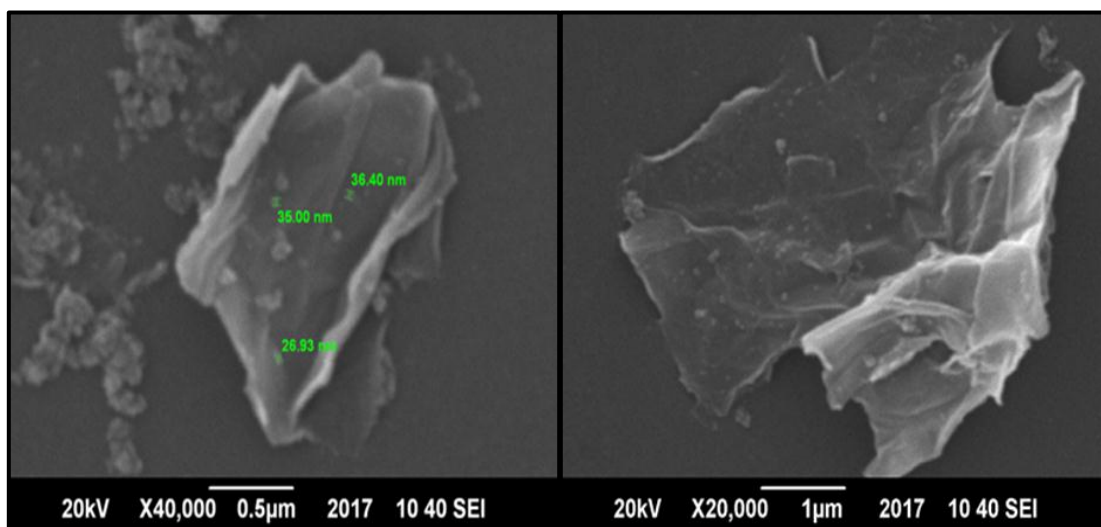
Figure 4.5 SEM analysis of NC-1
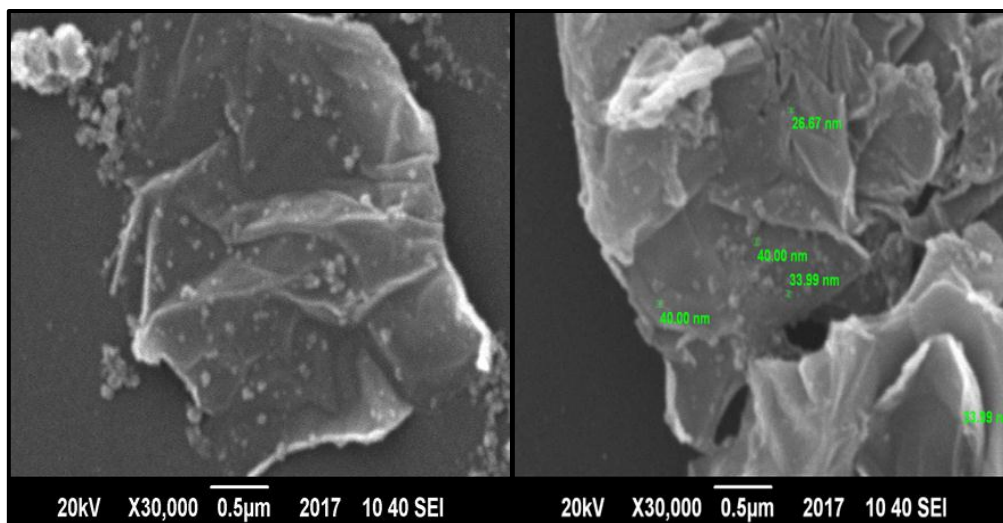
Figure 4.6 SEM analysis of NC-2
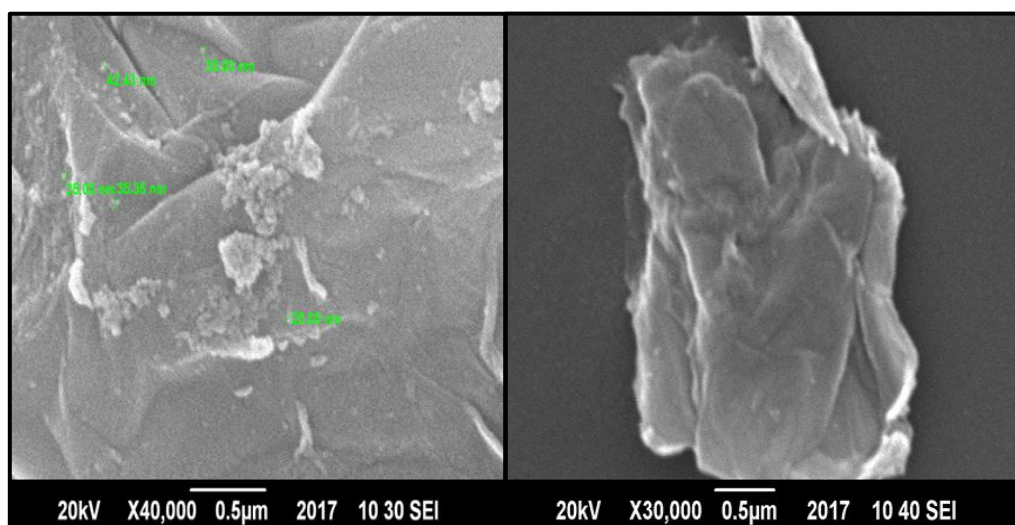
Figure 4.7 SEM analysis of NC-3

4.1.2. Energy dispersive X-ray spectroscopy (EDX)

EDX is used to determine composition of elements in a sample. Presence of every element in the sample is confirmed by its specific peak in the graph. The EDX results clearly show the signals for Titanium, oxygen, nitrogen and cobalt which are present in our synthesized samples. The EDX for undoped TiO_2 and co-doped TiO_2 is shown below.
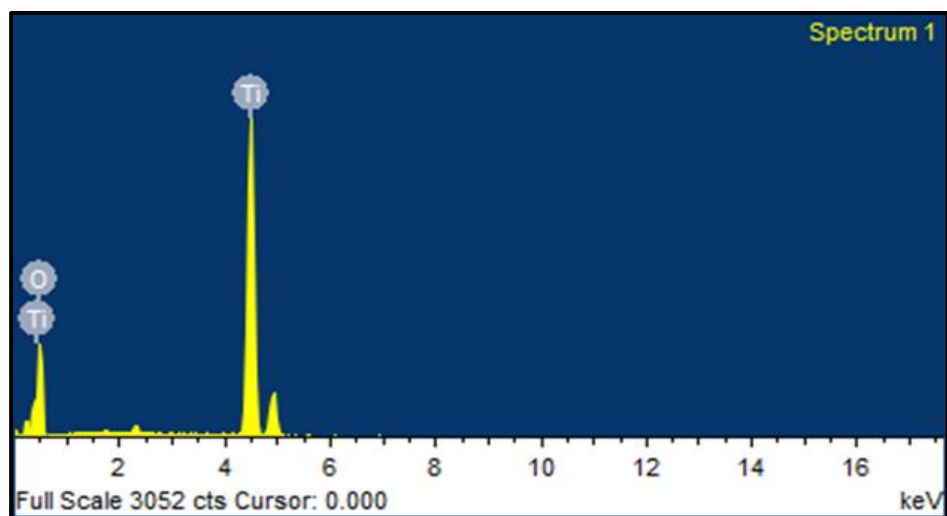
Figure 4.8 EDX spectra of TiO_2
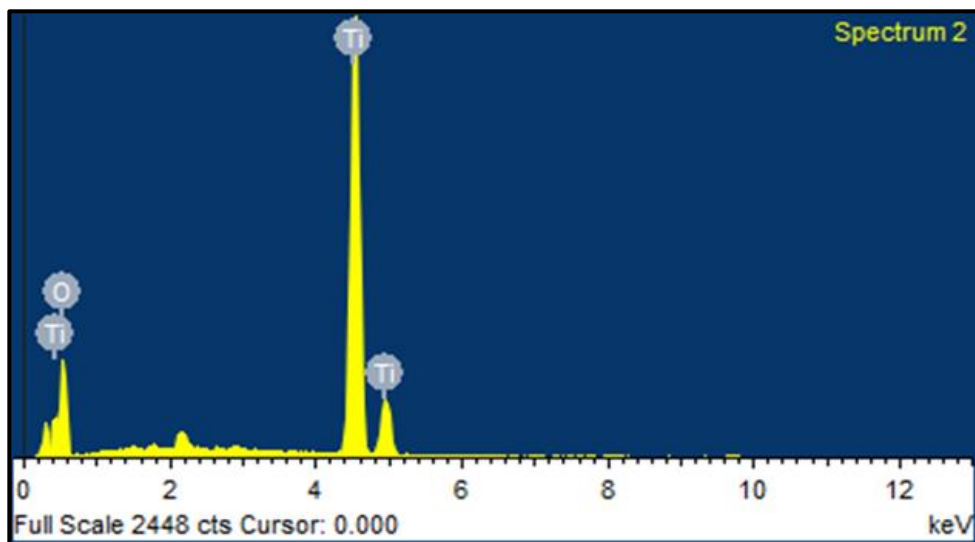
Figure 4.9 EDX spectra of N-TiO_2
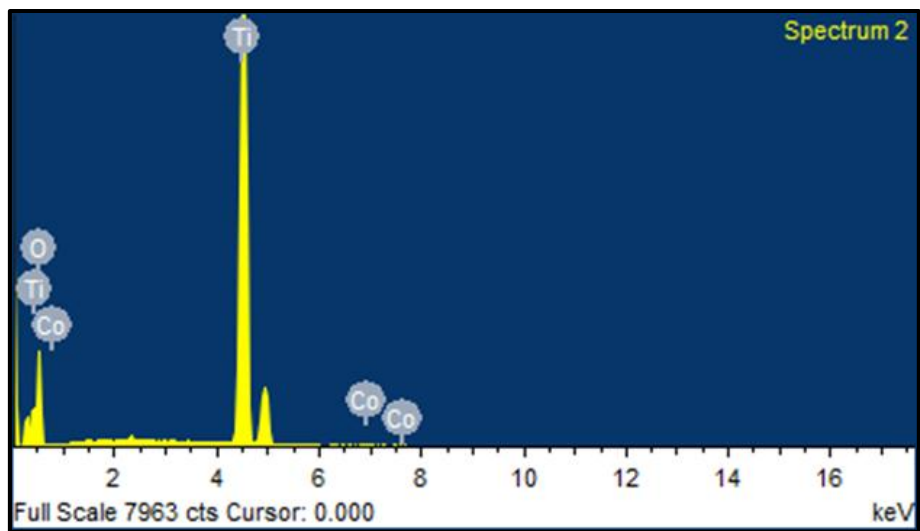
Figure 4.10 EDX spectra of CoN-TiO$_2$-1
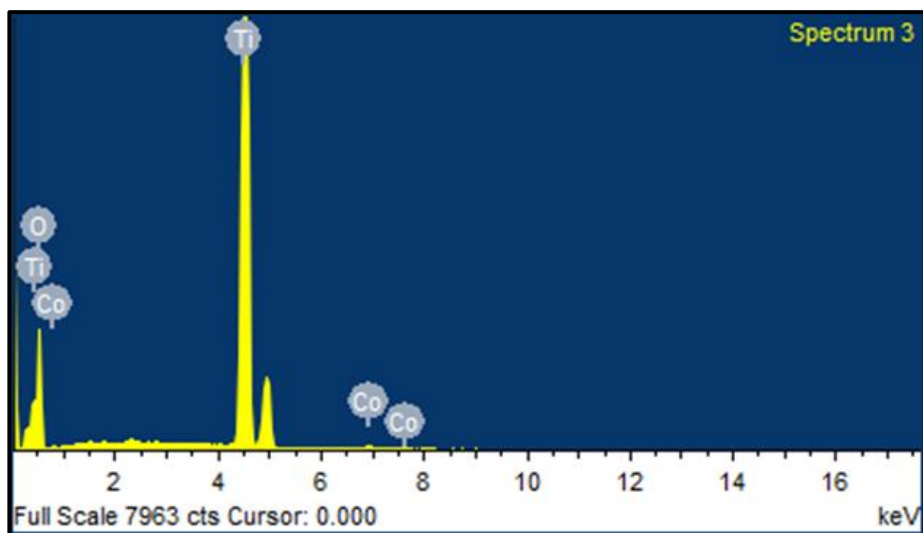
Figure 4.11 EDX spectra of CoN-TiO$_2$-2
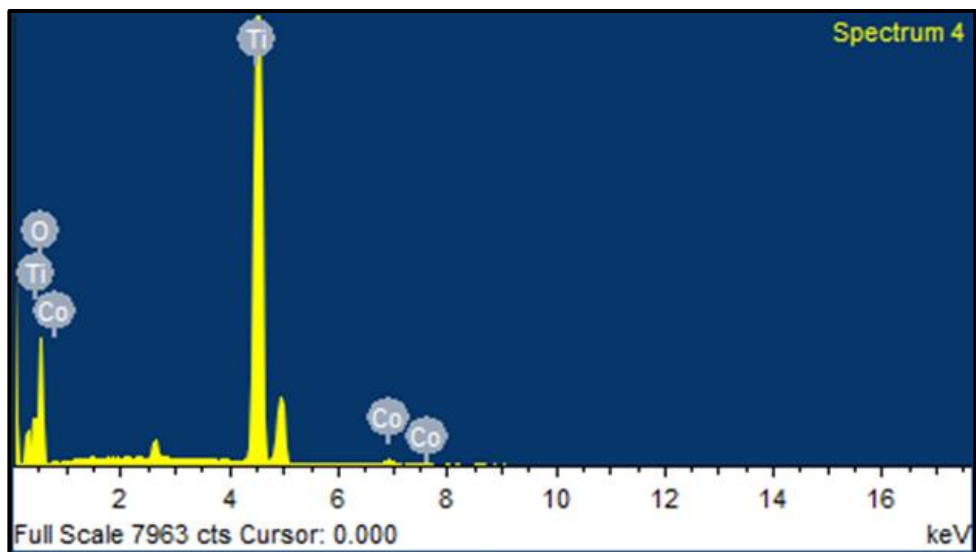
Figure 4.12 EDX spectra of CoN-TiO$_2$-3
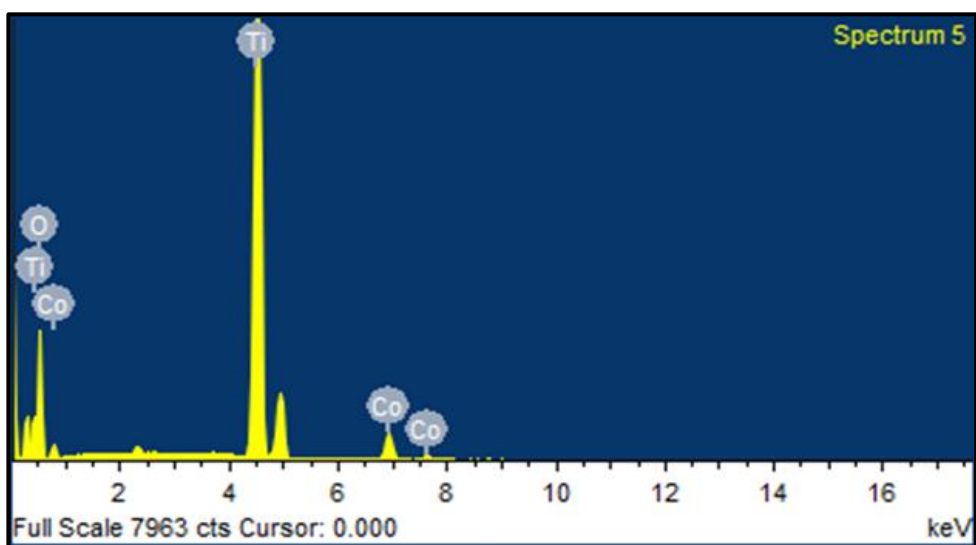
Figure 4.13 EDX spectra of CoN-TiO$_2$-4
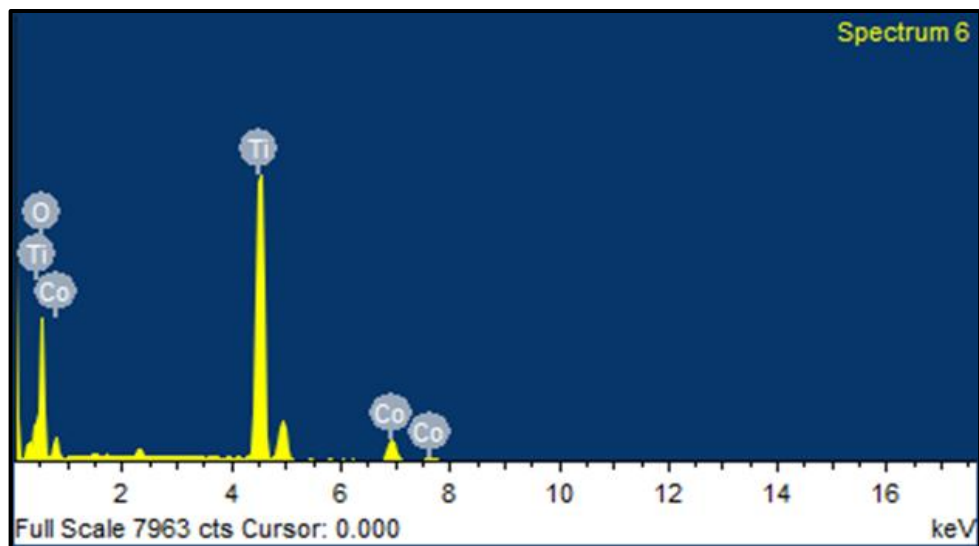
Figure 4.14 EDX spectra of CoN-TiO$_2$-5
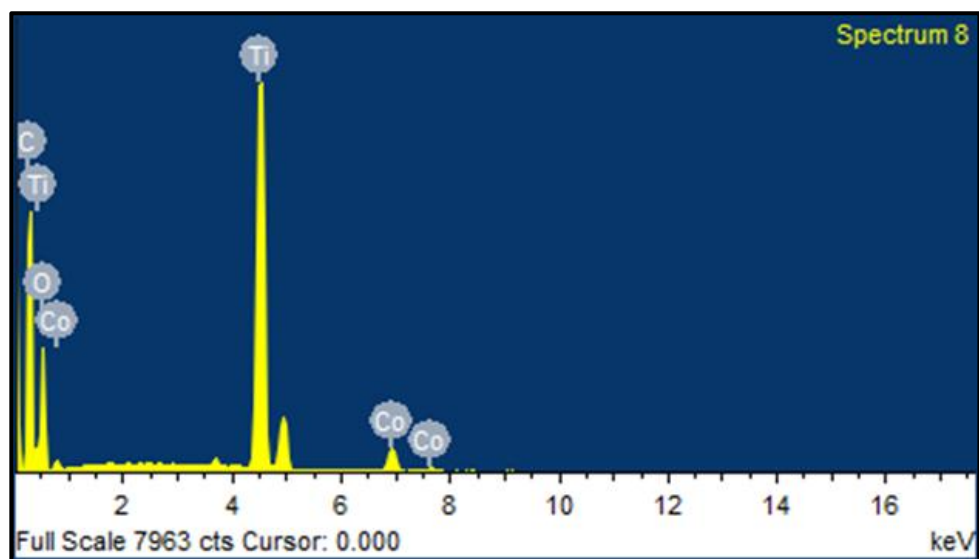
Figure 4.15 EDX spectra of NC-1
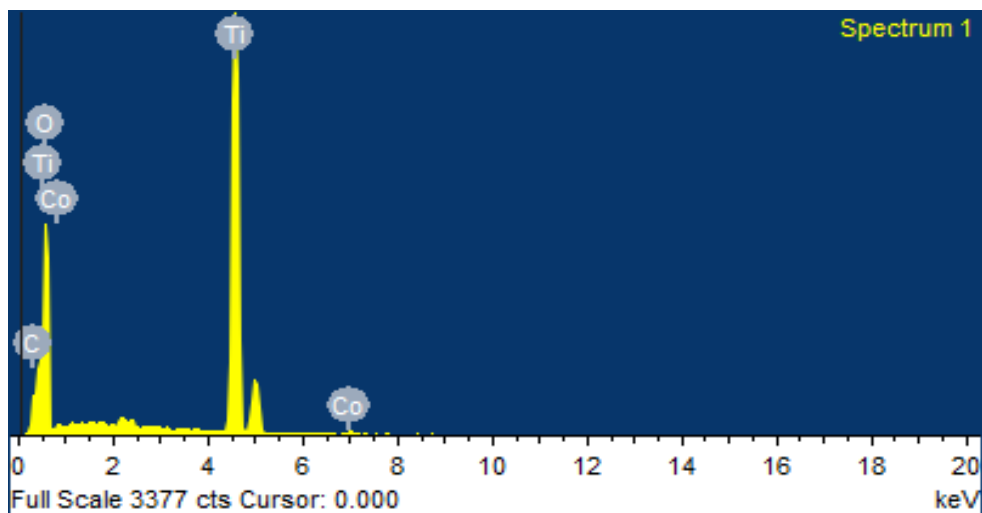
Figure 4.16 EDX spectra of NC-2
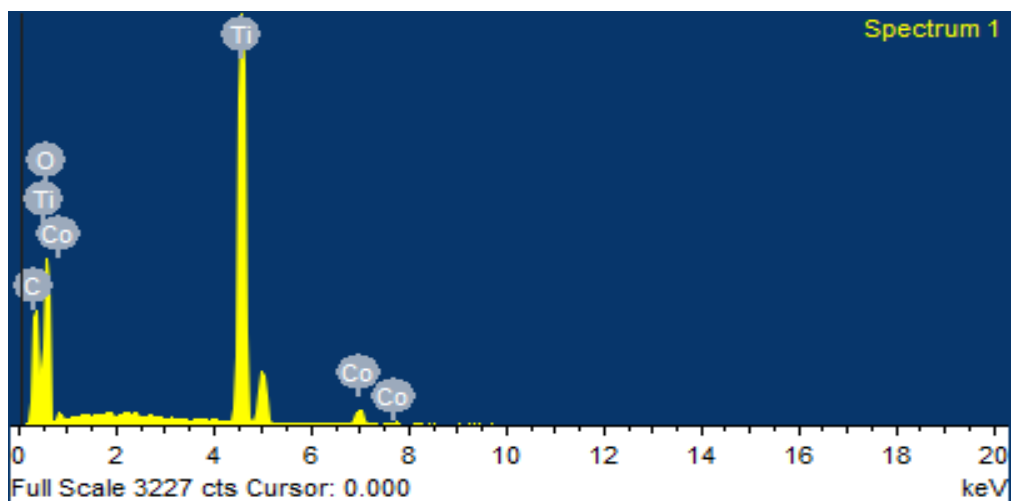
Figure 4.17 EDX spectra of NC-3

Table 4.1 Percentage composition of all elements in the synthesized catalysts

Sample Code	Atomic % of Ti	Atomic % of O	Atomic % of Co
TiO_2	24.33	75.77	----
$N-TiO_2$	12.93	87.07	----
$CoN-TiO_2-1$	27.83	72.03	0.13
$CoN-TiO_2-2$	27.26	72.46	0.27
$CoN-TiO_2-3$	25.75	73.65	0.60
$CoN-TiO_2-4$	18.07	79.23	2.70
$CoN-TiO_2-5$	24.60	72.64	2.76

Table 4.2 Percentage composition of all elements in Nanocomposites

Sample Code	Atomic % of C	Atomic % of O	Atomic % of Ti	Atomic % of Co
NC-1	25.16	35.48	35.05	4.31
NC-2	35.72	40.79	19.01	4.48
NC-3	40.81	44.43	10.36	4.40

4.1.3. Diffuse reflectance spectroscopy and Tauc plots

DRS Spectras were used for the construction of tauc plots to calculate band gap from them. Anatase TiO_2 has a band gap of 3.2 eV and that's why it absorbs UV light only. Doping of TiO_2 reduces its band gap and extends its absorption in visible region. Tauc Plots of all the prepared catalysts are shown below.
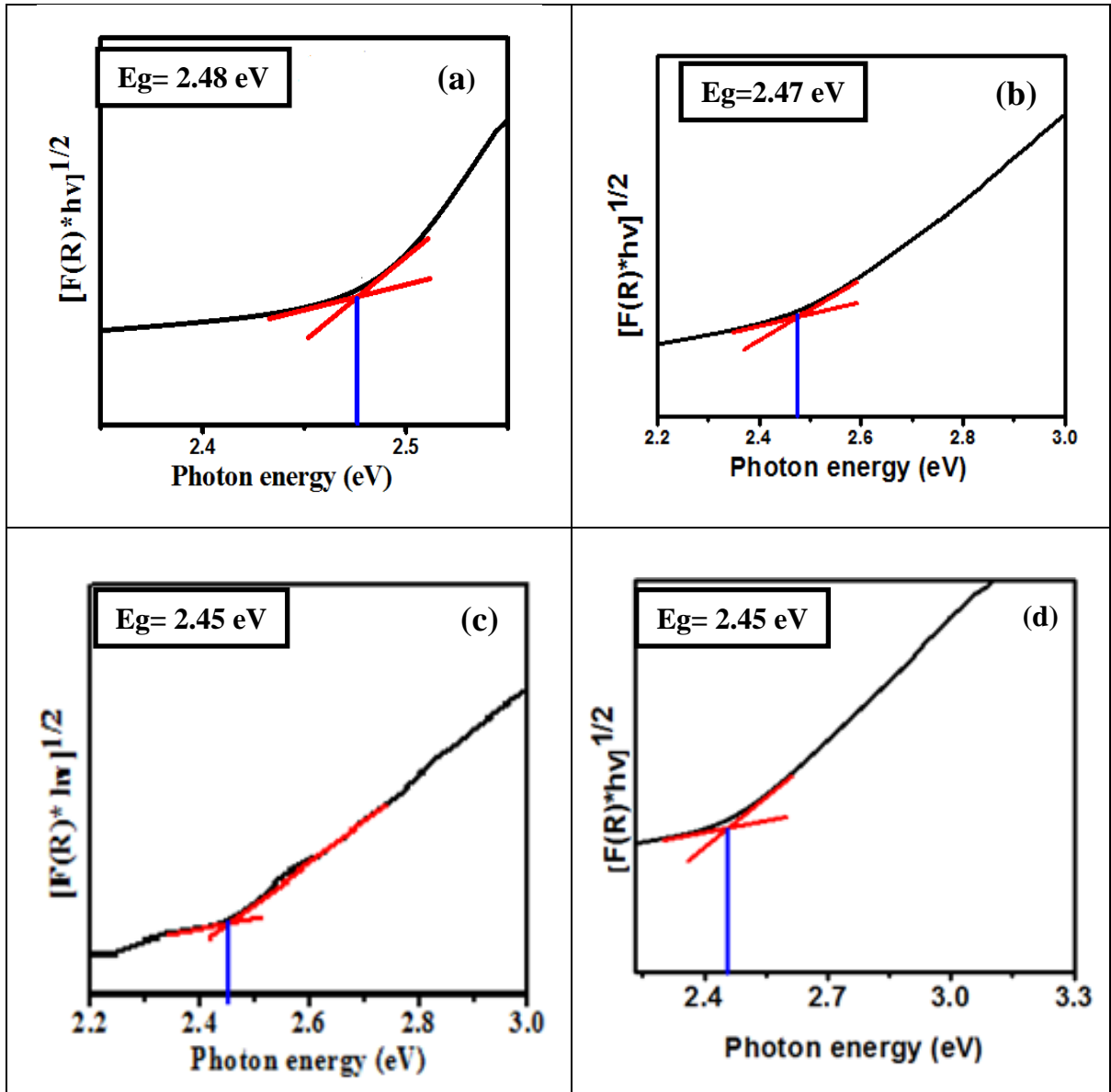
Figure 4.18 Tauc plots of (a) N-TiO$_2$ (b) CoN-TiO$_2$-1 (c) CoN-TiO$_2$-2 (d) CoN-TiO$_2$-3
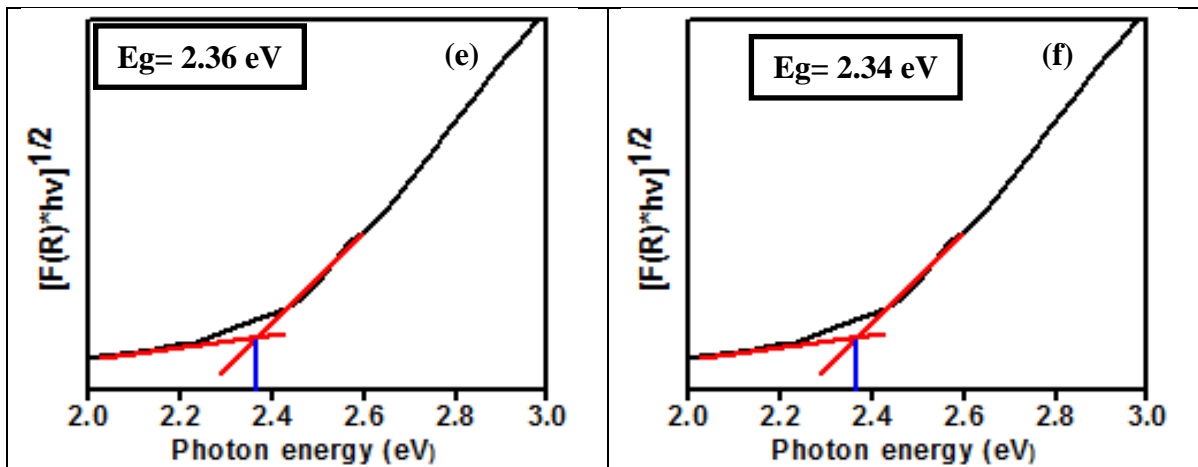
Figure 4.19 Tauc plots of (e) CoN-TiO$_2$-4 (f) CoN-TiO$_2$-5

Tauc plots of nanocomposites also showed a significant reduction in and band gap as shown below.
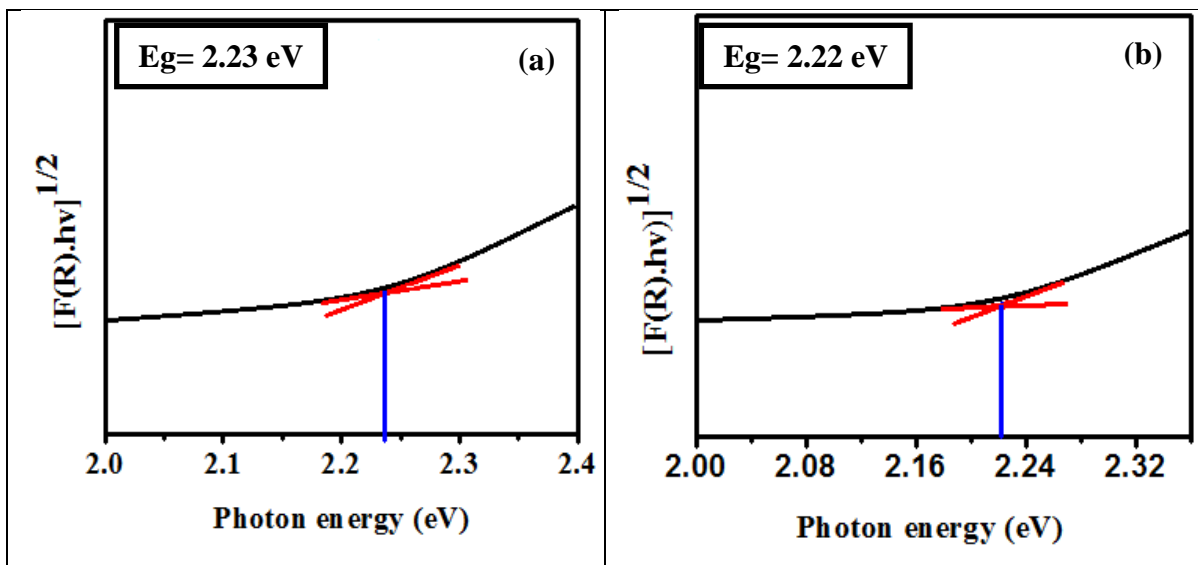
Figure 4.20 Tauc plots of (a) NC-1 (b) NC-2
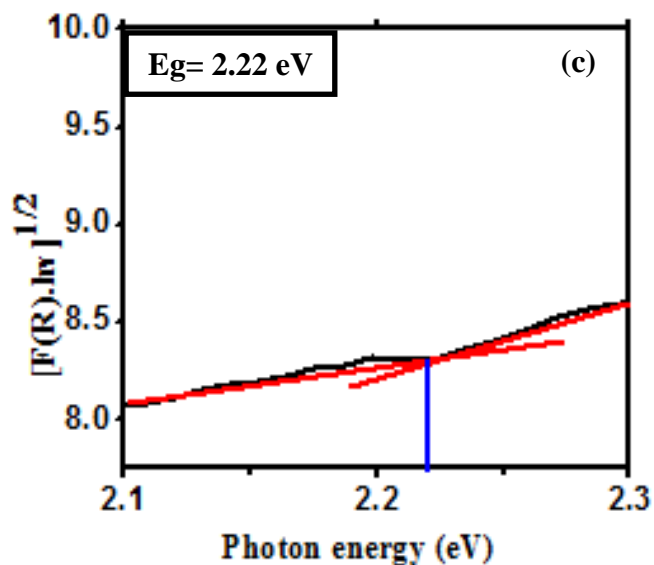
Figure 4.21 Tauc plot of (c) NC-3

Table 4.3 Band gaps of prepared samples

Sample code	Band gap (eV)
TiO_2	3.21
$N-TiO_2$	2.48
$CoN-TiO_2-1$	2.47
$CoN-TiO_2-2$	2.47
$CoN-TiO_2-3$	2.45
$CoN-TiO_2-4$	2.36
$CoN-TiO_2-5$	2.34
NC-1	2.23
NC-2	2.22
NC-3	2.22

4.1.4. X-Ray diffraction (XRD)

JEOL-JDX- II, X-ray diffractometer was used for XRD analysis. The matching of XRD patterns with standard reference codes (96-900-908214 to 96-900-908214) was carried out by using X'Pert High score plus. All the synthesized samples showed their diffraction

peaks at 25.3 ° , 37.8 °, 48.06 °, 55.1 ° and 62.7 ° having their lattice planes (101), (004), (200), (105), and (204) which were matched with the standard JCPDS cards showing that all the doped and co-doped catalysts have tetragonal structure and anatase phase. There were no nitrogen or cobalt related peaks observed as the dopants were used in a very low concentration.
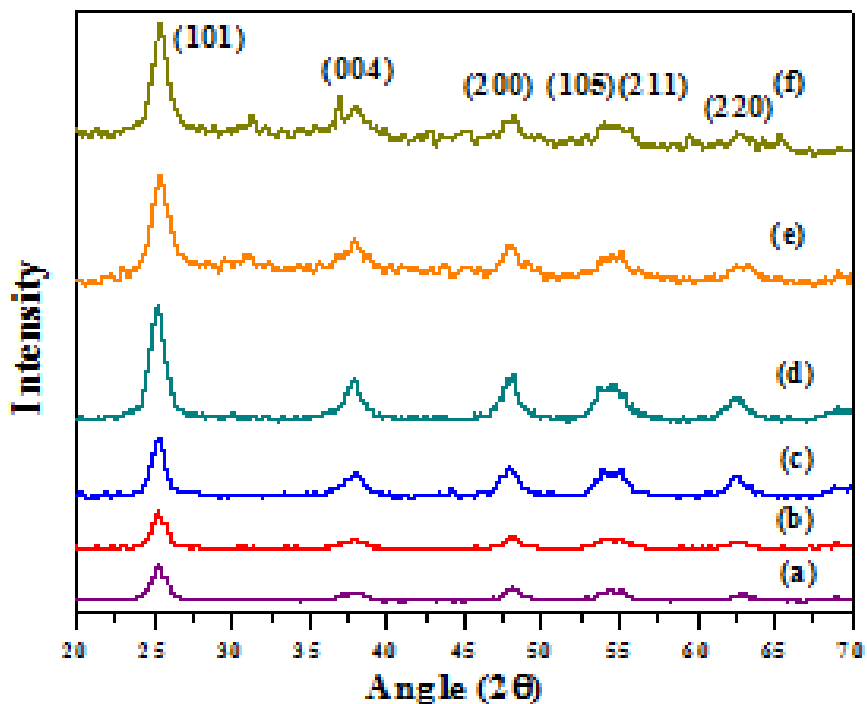
Figure 4.22 XRD patterns of (a) TiO_2 (b) $N-TiO_2$ (c) $CoN-TiO_2-1$ (d) $CoN-TiO_2-2$ (e) $CoN-TiO_2-3$ (f) $CoN-TiO_2-4$ (g) $CoN-TiO_2-5$

XRD pattern of graphene oxide shows a diffraction peak at $2\theta=10°$ corresponding to the diffraction plane (001), which shows that graphite has been successfully oxidized. Appearance of

A small peak at $2\theta=25°$ shows the presence of some amount of unreacted graphite.
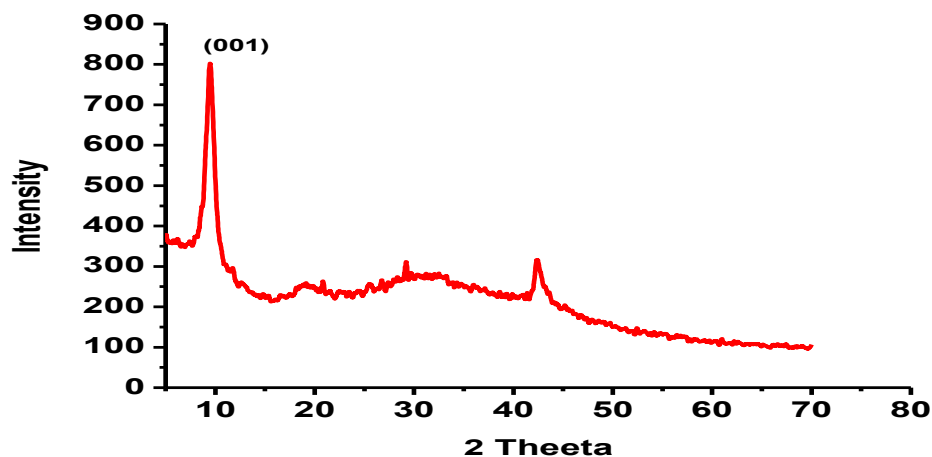
Figure 4.23 XRD pattern of graphene oxide

The XRD Patters of nanocomposites have been shown in the figure below. These XRD Patterns show that nanocomposites don't show any peak at $2\theta=10°$ which means that graphene oxide has been reduced during the formation of nanocomposite. No characteristic peak of RGO has been observed which may be because of overlapping of (101) peak of TiO_2 with the characteristic peak of RGO at $2\theta=25°$ All of these nanocomposites show characteristic peaks at 25.3 ° , 37.4 °, 48.07 °, 55.4 ° and 62.7 ° which correspond to lattice planes (101), (004), (200), (211), (204). The presence of these peaks shows the presence of pure anatase phase.
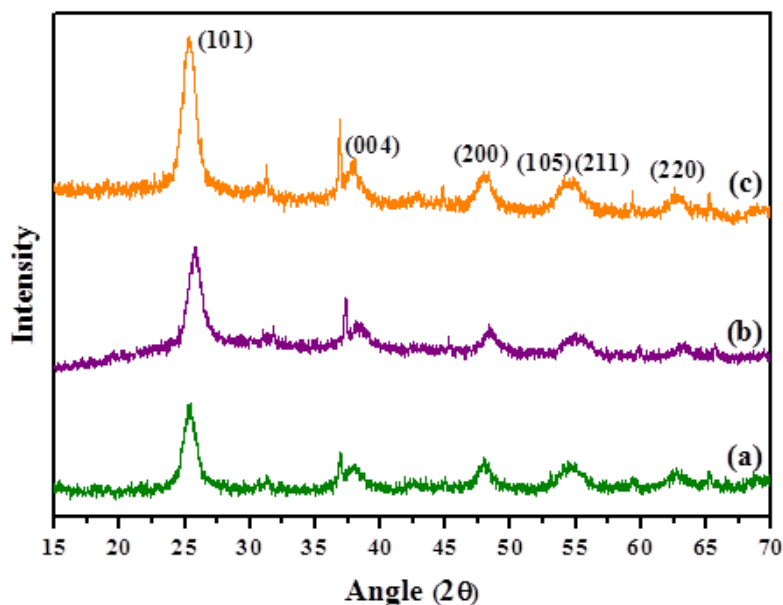
Figure 4.24 XRD patterns of (a) NC-1 (b) NC-2 (c) NC-3

Crystallite sizes of all the catalysts were determined by using Scherrer formula $(D=K\lambda/(\beta \cos \theta)$ [120]. The crystallite sizes of all the catalysts have been shown in the table below.

Table 4.4 Crystallite sizes of all the catalysts calculated by Scherrer formula

Sample Code	Crystallite size (nm)
TiO_2	26
$N\text{-}TiO_2$	13.5
$CoN\text{-}TiO_2\text{-}1$	10
$CoN\text{-}TiO_2\text{-}2$	10
$CoN\text{-}TiO_2\text{-}3$	9.7
$CoN\text{-}TiO_2\text{-}4$	8.75
$CoN\text{-}TiO_2\text{-}5$	8

4.1.5. Brunauer Emmett-Teller (BET) surface area analysis

BET analysis of the samples was carried out to determine the surface area. The surface area of undoped TiO_2 is very less whereas doping increases the surface area of the nanoparticles. Following table shows the surface area of the synthesized catalysts of which $CoN\text{-}TiO_2\text{-}5$ shows the highest surface because of increased dopant concentration.

Table 4.5 BET surface area of different catalysts

Sample Code	BET surface area (m^2/g)
Undoped TiO_2	11
$CoN\text{-}TiO_2\text{-}2$	57.49
$CoN\text{-}TiO_2\text{-}4$	62.08
$CoN\text{-}TiO_2\text{-}5$	63.23

4.1.6. Fourier transform infrared spectroscopy (FT-IR)

Figure shows FT-IR spectra of all the prepared catalysts. These spectras give information about the attached functional groups. A FT-IR spectrum of graphene oxide shows prominent peaks at 1040 cm^{-1}, 1200 cm^{-1}, 1410 cm^{-1} and 1720 cm^{-1}. These peaks correspond to strong stretching vibrations of oxygen containing functional groups alkoxy (C-O), epoxy (C-O), carboxyl (C=O) and carboxyl (C-O) respectively. The intensities of these peaks were significantly reduced in nanocomposites which shows that GO has been reduced during the formation of nanocomposite. A strong absorption peak between 3000-3500 cm^{-1} shows the stretching vibration of surface hydroxyl groups. In nanocomposites a peak at ~1220 cm^{-1} is present which is because of Ti-O-C bond [121]. The presence of this peak shows the formation of nanocomposite. A new peak at ~1570 cm^{-1} is related to the skeletal vibration of RGO sheets [121]. A small shoulder peak at ~1650 shows the stretching vibrations of C=O bond [122].
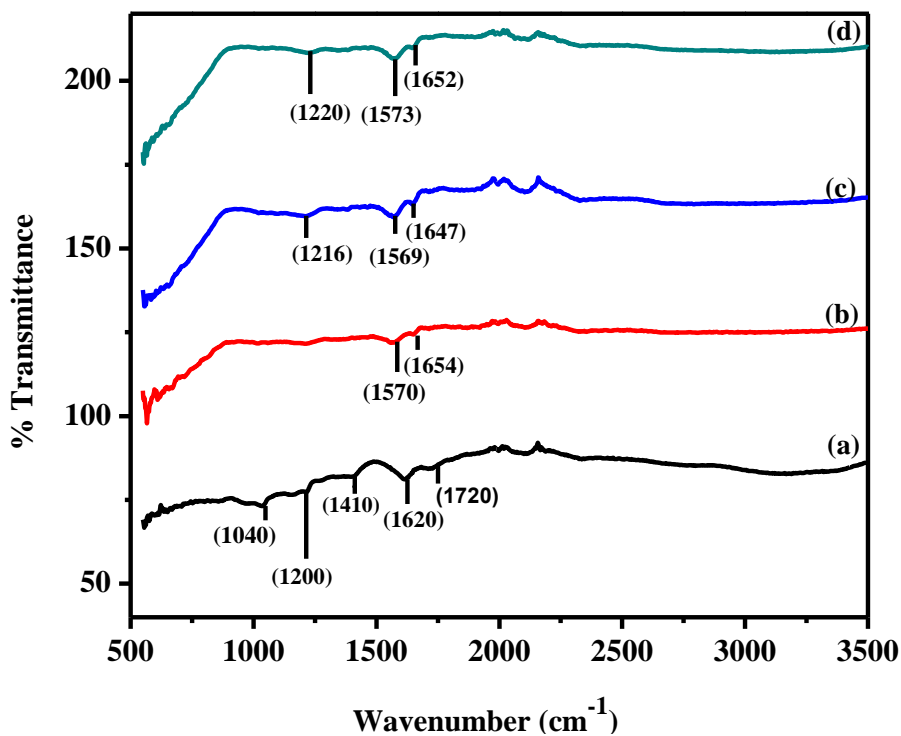
Figure 4.25 FT-IR spectras of (a) GO (b) NC-1 (c) NC-2 (d) NC-3

4.2. Degradation experiment

4.2.1. Investigation of photocatalytic activity of the synthesized catalysts against methyl orange

The as prepared catalysts were used for the photocatalytic degradation of methyl orange. Pure methyl orange was used. A solution of 0.1 mM was prepared in distilled water as a stock solution. This solution was further diluted to 0.01 mM. For the photocatalytic experiment 50 ml solution was taken in a conical flask to which 50 mg catalyst was added. These solutions were allowed to stir for two hours to ensure adsorption-desorption equilibrium. Then solutions were kept under LED lamp with continuous stirring. All the experiments were performed at room temperature. 5 mL aliquots were taken after every hour and after centrifugation, their absorbance was measured by using UV-vis spectrophotometer. The decrease in absorbance showed that concentration of methyl orange was also decreasing.

4.2.1.1. Degradation of methyl orange in dark and visible light

Degradation of methyl orange in dark is low as compared to its degradation under visible light. A comparison of photocatalytic activities of the catalysts under visible light and dark has been shown below.
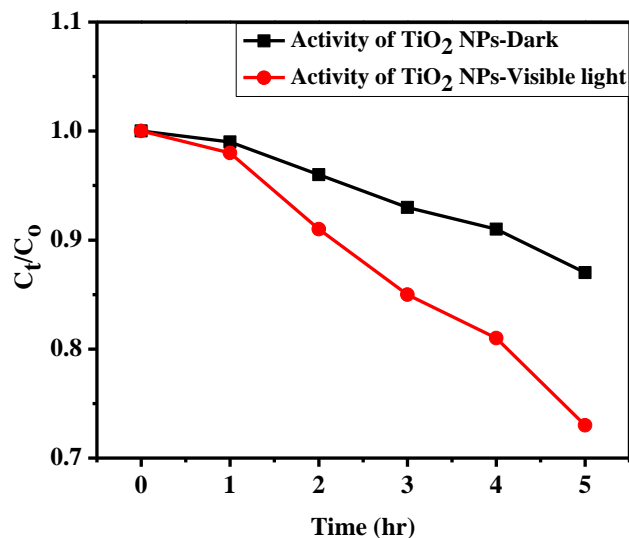
Figure 4.26 Activity of TiO$_2$ nanoparticles against methyl orange degradation in dark and visible light
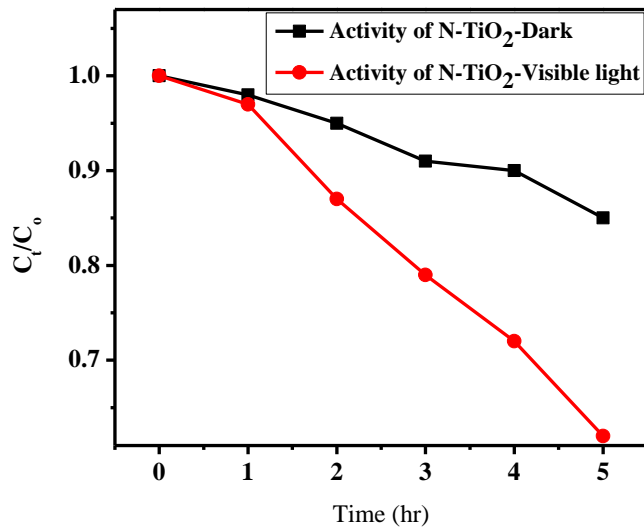
Figure 4.27 Activity of N-TiO$_2$ against methyl orange degradation in dark and visible light
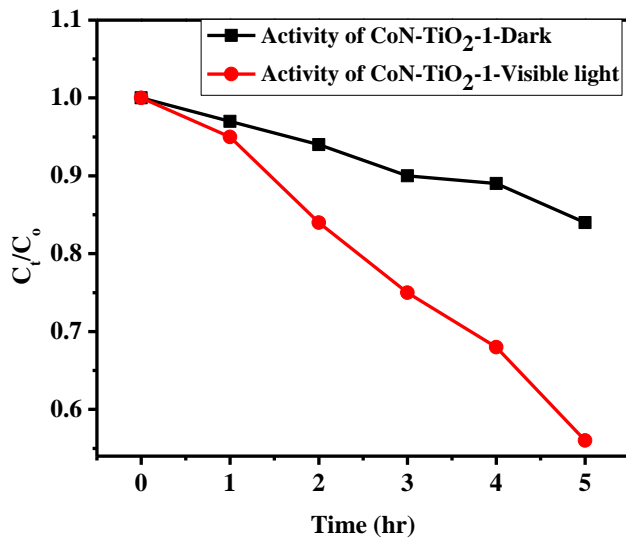
Figure 4.28 Activity of CoN-TiO$_2$-1 against methyl orange degradation in dark and visible light
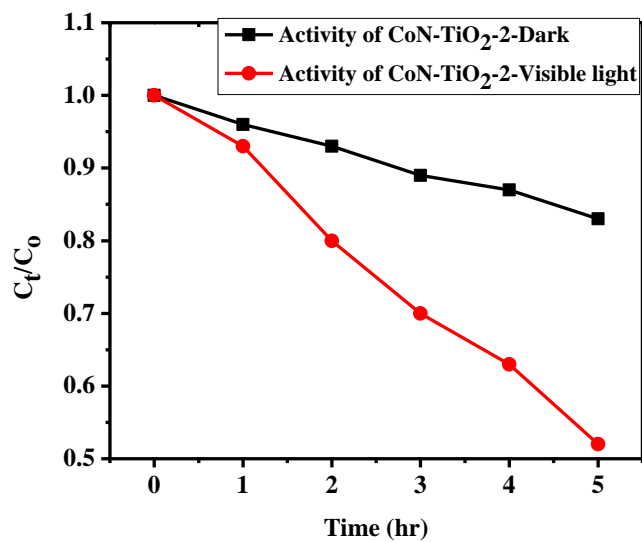
Figure 4.29 Activity of CoN-TiO$_2$-2 against methyl orange degradation in dark and visible light
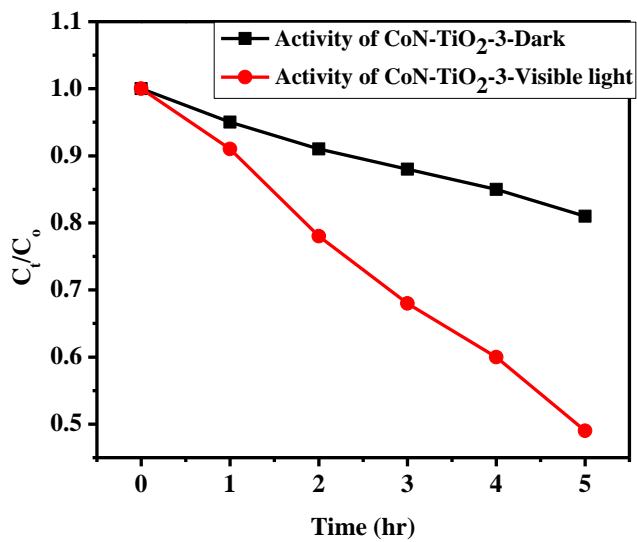
Figure 4.30 Activity of CoN-TiO$_2$-3 against methyl orange degradation in dark and visible light
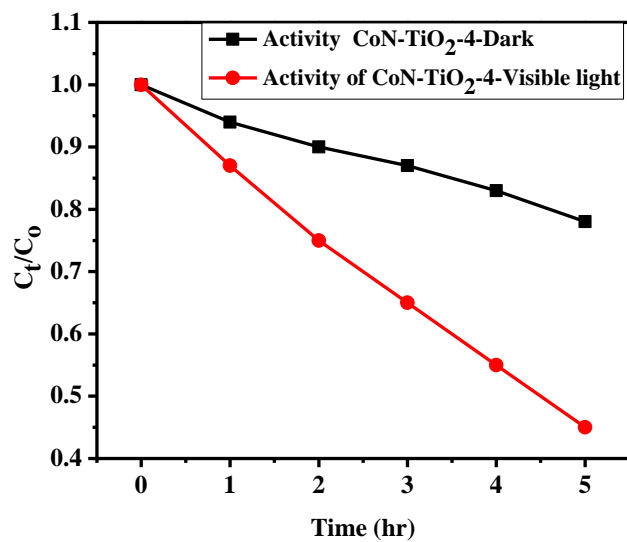
Figure 4.31 Activity of CoN-TiO$_2$-4 against methyl orange degradation in dark and visible light
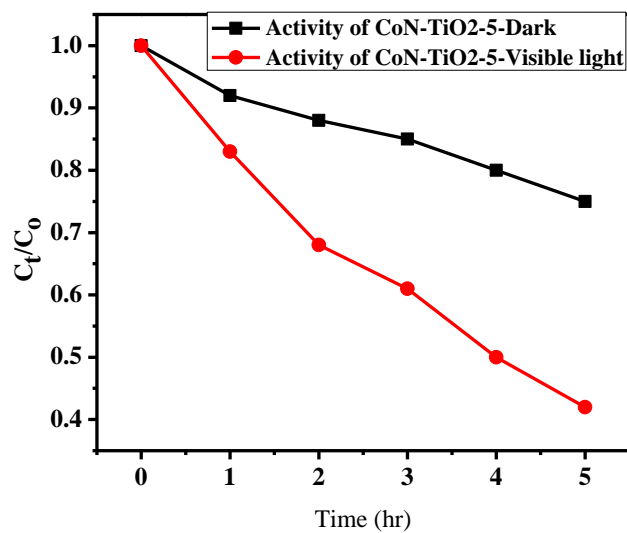
Figure 4.32 Activity of CoN-TiO$_2$-5 against methyl orange degradation in dark and visible light
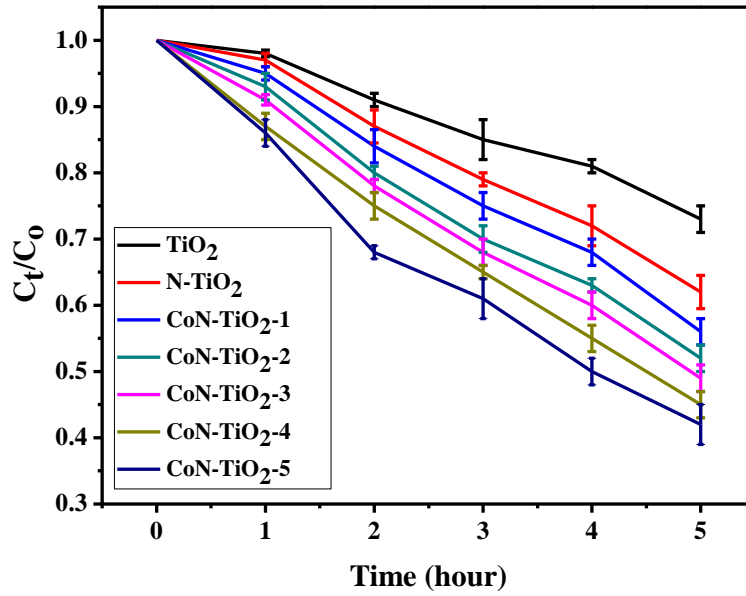
Figure 4.33 Activity of all catalysts against methyl orange degradation in visible light
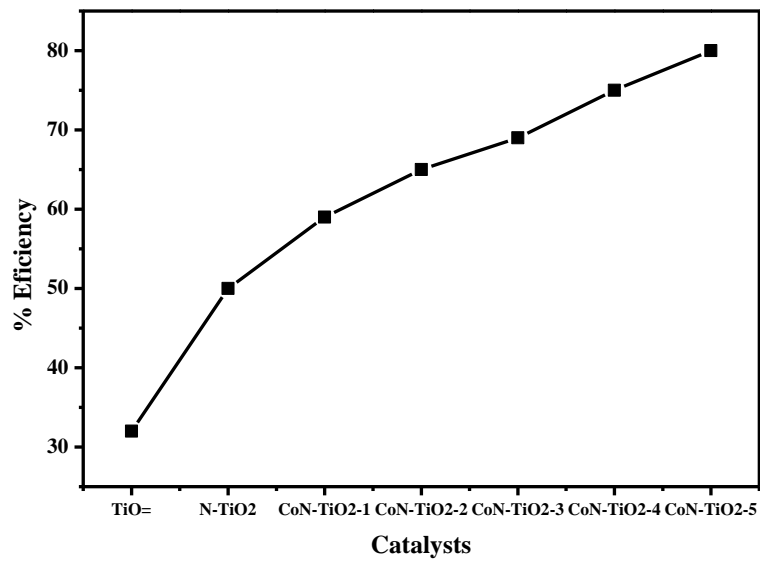
Figure 4.34 Comparison of percentage efficiency of all catalysts against methyl orange in visible light
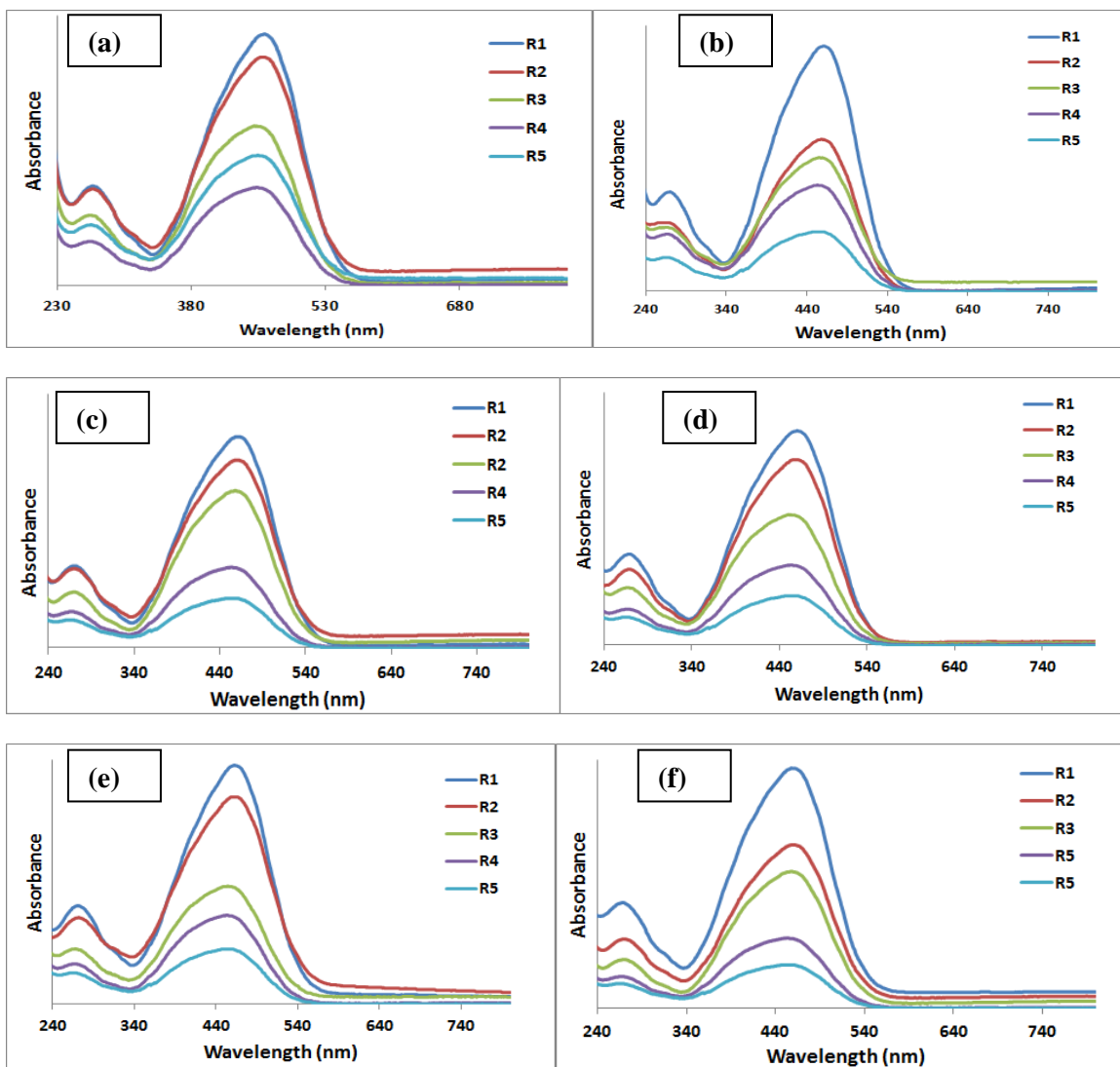
Figure 4.35 Degradation graphs of methyl orange by using (a) undoped TiO_2 (b) N-TiO_2 (c) CoN-TiO_2-1 (d) CoN-TiO_2-2 (e) CoN-TiO_2-3 (f) CoN-TiO_2-4
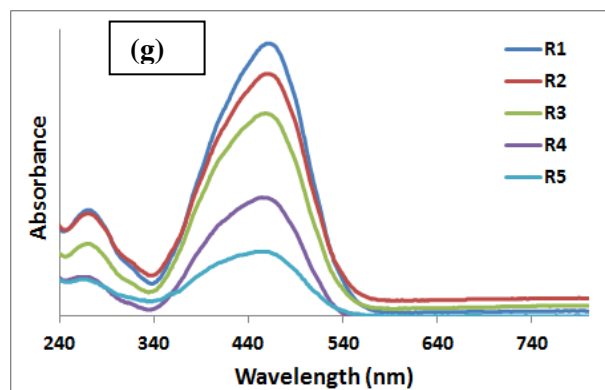
Figure 4.36 Degradation graph of methyl orange by using (g) CoN-TiO$_2$-5

Activity of all doped and co-doped catalysts was found to be higher than undoped TiO$_2$ nanoparticles because doping of TiO$_2$ shifts absorption in the visible region and increases its photocatalytic activity. N, Co-TiO$_2$ showed better photocatalytic activity than N-TiO$_2$ as cobalt doping can further increase the absorption of visible light. Among co-doped catalysts CoN-TiO$_2$-5 showed highest photocatalytic activity as it has highest concentration of dopant and also it has high surface area. High surface area means increased number of active sites which lead to increased adsorption of methyl orange and hence more photodegradation will result.

As CoN-TiO$_2$-5 was the best catalyst so it was selected for the synthesis of nanocomposites with graphene oxide. Three nanocomposites having ratio of N, Co-TiO$_2$: GO 1:1, 1:2, 1:3 were prepared and were used for the photocatalytic degradation of visible light.
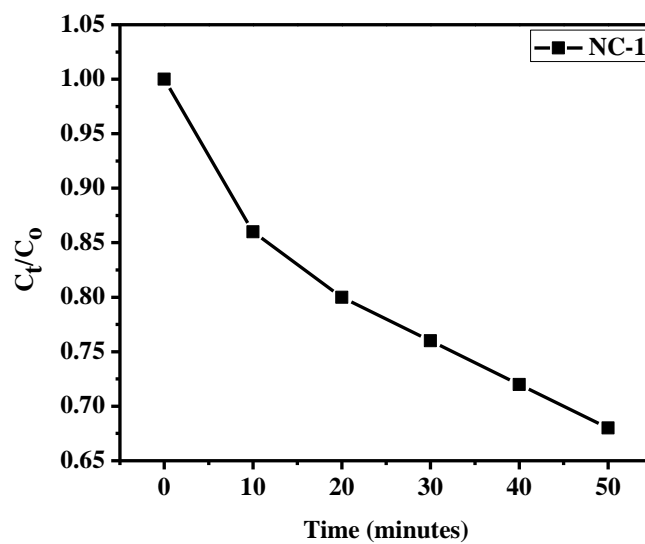
Figure 4.37 Activity of NC-1 against methyl orange degradation in visible light
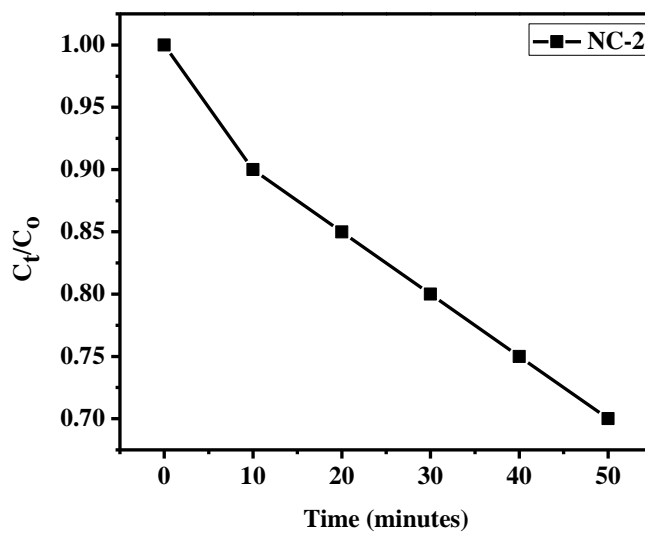
Figure 4.38 Activity of NC-2 against methyl orange degradation in visible light
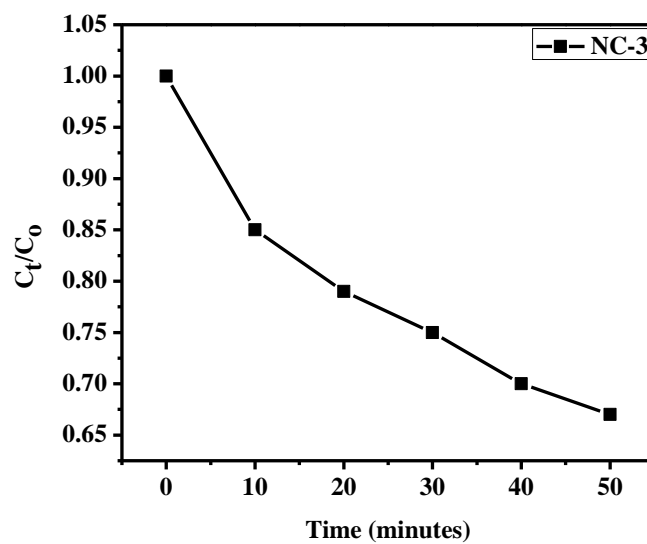
Figure 4.39 Activity of NC-3 against methyl orange degradation in visible light
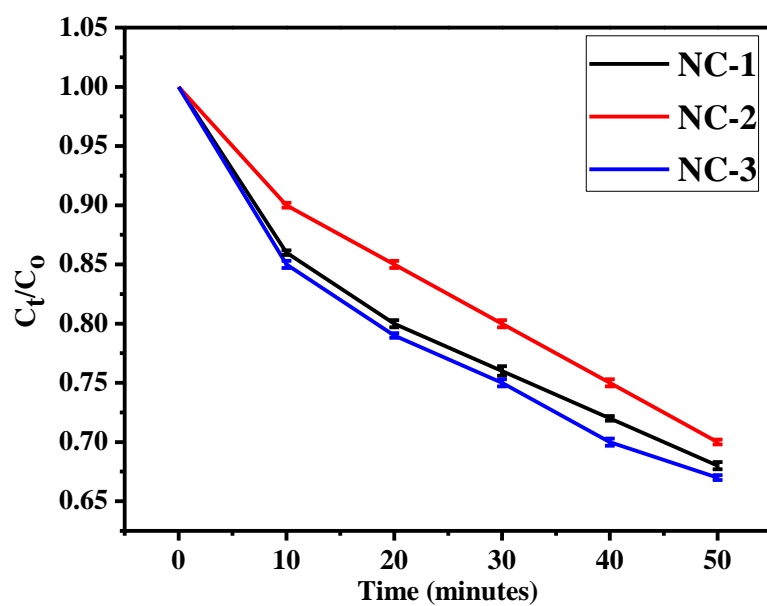
Figure 4.40 Activity of all nanocomposites against methyl orange degradation in visible light
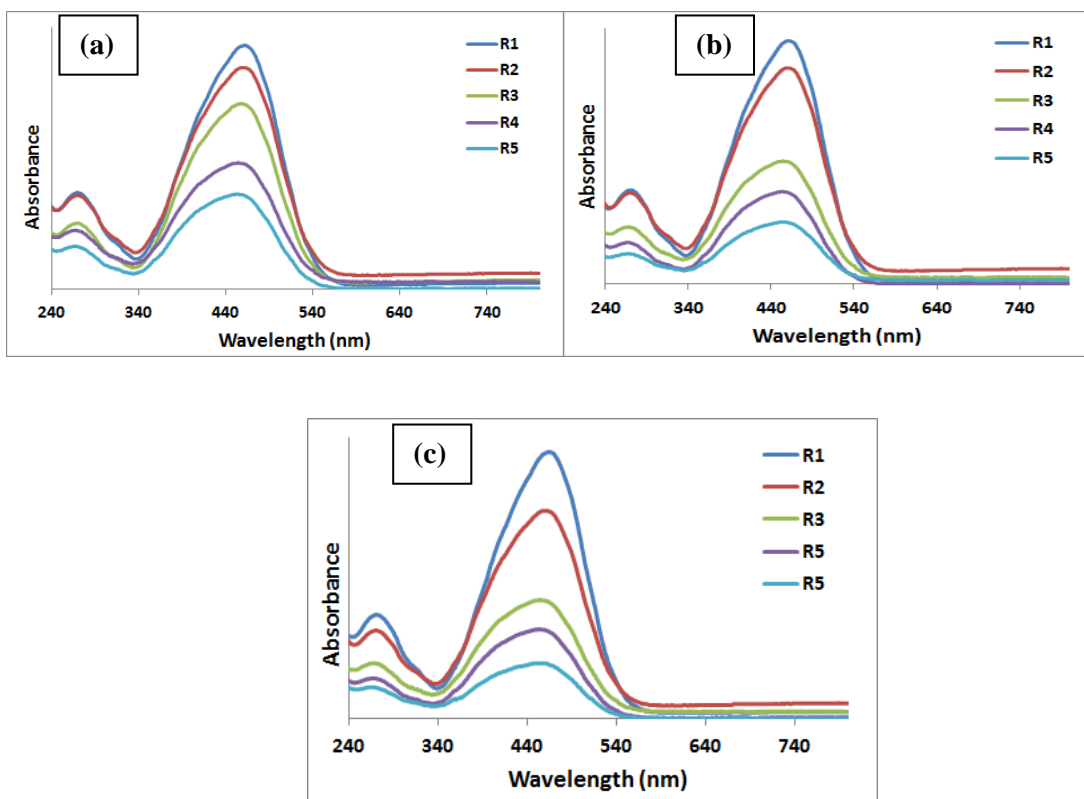
Figure 4.41 Degradation graphs of methyl orange using (a) NC-1 (b) NC-2 (c) NC-3
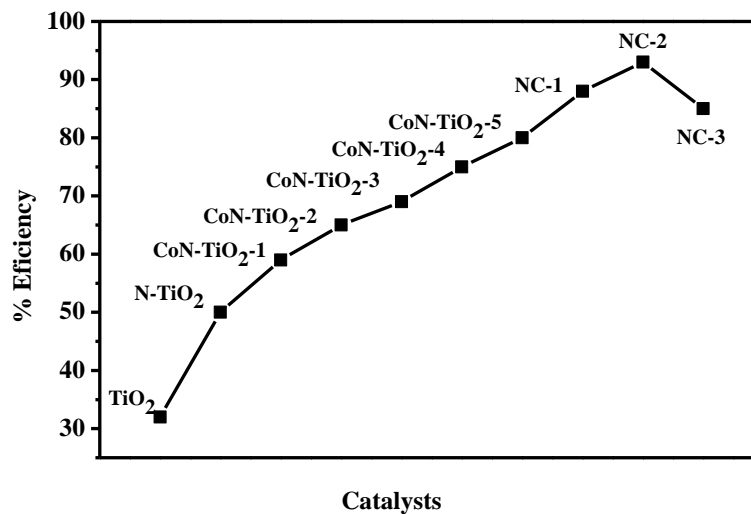
Figure 4.42 Comparison of percentage efficiency of all catalysts against methyl orange degradation in visible light

Table 4.6 Degradation rate calculation for methyl orange from the absorbance recorded (in dark)

Catalyst	Time (hr)	Absorbance Examined	C_t	C_o	C_t/C_o	ln C_t/C_o	Negative of ln C_t/Co
TiO₂ nanoparticles	1	0.65	1.66		0.99	-0.01	0.01
	2	0.62	1.61		0.96	-0.04	0.04
	3	0.60	1.56		0.93	-0.07	0.07
	4	0.58	1.53		0.91	-0.09	0.09
	5	0.54	1.46	1.68	0.87	-0.14	0.14
N-TiO₂	1	0.63	1.62		0.98	-0.02	0.02
	2	0.6	1.56		0.95	-0.05	0.05
	3	0.56	1.49		0.91	-0.09	0.09
	4	0.55	1.47		0.90	-0.11	0.11
	5	0.51	1.39	1.64	0.85	-0.16	0.16
CoN-TiO₂-1	1	0.60	1.57		0.97	-0.03	0.03
	2	0.58	1.52		0.94	-0.06	0.06
	3	0.55	1.47		0.90	-0.11	0.11
	4	0.54	1.45		0.89	-0.12	0.12
	5	0.49	1.36	1.62	0.84	-0.17	0.17
CoN-TiO₂-2	1	0.59	1.55		0.96	-0.04	0.04
	2	0.57	1.51		0.93	-0.07	0.07
	3	0.54	1.45		0.89	-0.12	0.12
	4	0.52	1.41		0.87	-0.14	0.14
	5	0.48	1.34	1.62	0.83	-0.19	0.19
CoN-TiO₂-3	1	0.58	1.52		0.95	-0.05	0.05
	2	0.54	1.46		0.91	-0.09	0.09
	3	0.52	1.41		0.88	-0.13	0.13
	4	0.49	1.36		0.85	-0.16	0.16
	5	0.46	1.30	1.60	0.81	-0.21	0.21
CoN-TiO₂-4	1	0.55	1.47		0.94	-0.06	0.06
	2	0.51	1.40		0.90	-0.11	0.11
	3	0.49	1.36		0.87	-0.14	0.14
	4	0.46	1.30		0.83	-0.19	0.19
	5	0.42	1.22	1.56	0.78	-0.25	0.25
	1	0.50	1.37		0.92	-0.08	0.08

Catalyst	Time (hr)	Absorbance	C_t	C_o	C_t/C_o	ln C_t/C_o	Negative of ln C_t/C_o
	2	0.47	1.31		0.88	-0.13	0.13
	3	0.44	1.27		0.85	-0.16	0.16
	4	0.41	1.20		0.80	-0.22	0.22
CoN-TiO$_2$-5	5	0.36	1.11	1.49	0.75	-0.29	0.29

Table 4.7 Degradation rate calculation for MO degradation under visible light

Catalyst	Time (hr)	Absorbance	C_t	C_o	C_t/C_o	ln C_t/C_o	Negative of ln C_t/C_o
TiO$_2$ nanoparticles	1	0.64	1.64		0.98	- 0.02	-0.02
	2	0.58	1.53		0.91	- 0.09	0.09
	3	0.53	1.43	1.68	0.85	- 0.16	0.16
	4	0.49	1.36		0.81	- 0.21	0.21
	5	0.45	1.23		0.73	- 0.31	0.31
N-TiO$_2$	1	0.62	1.60		0.97	- 0.02	0.02
	2	0.53	1.43		0.87	- 0.14	0.14
	3	0.46	1.3	1.64	0.79	- 0.24	0.24
	4	0.41	1.2		0.72	- 0.33	0.33
	5	0.32	1.02		0.62	- 0.48	0.48
CoN-TiO$_2$-1	1	0.59	1.54		0.95	- 0.05	0.05
	2	0.49	1.36		0.84	- 0.13	0.13
	3	0.42	1.22	1.62	0.75	- 0.24	0.24
	4	0.36	1.10		0.68	- 0.38	0.38
	5	0.26	0.91		0.56	- 0.58	0.58
CoN-TiO$_2$-2	1	0.57	1.51		0.93	- 0.08	0.08
	2	0.46	1.30		0.80	- 0.22	0.22
	3	0.37	1.13	1.62	0.70	- 0.42	0.42
	4	0.32	1.02		0.63	- 0.56	0.56
	5	0.22	0.84		0.52	- 0.65	0.65
CoN-TiO$_2$-3	1	0.54	1.45		0.91	- 0.07	0.07
	2	0.44	1.25		0.78	- 0.25	0.25
	3	0.35	1.08	1.60	0.68	- 0.38	0.38
	4	0.28	0.95		0.60	- 0.51	0.51
	5	0.19	0.78		0.49	- 0.71	0.71
	1	0.53	1.43		0.87	- 0.10	0.10
	2	0.39	1.17		0.75	- 0.28	0.28

Catalyst	Time						
CoN-TiO$_2$-4	3	0.32	1.02	1.56	0.65	- 0.43	0.43
	4	0.23	0.86		0.55	- 0.60	0.60
	5	0.15	0.70		0.45	- 0.80	0.80
CoN-TiO$_2$-5	1	0.45	1.28		0.86	- 0.15	0.15
	2	0.31	1.01		0.68	- 0.38	0.38
	3	0.26	0.91	1.49	0.61	- 0.49	0.49
	4	0.17	0.74		0.50	- 0.7	0.7
	5	0.11	0.63		0.42	- 0.87	0.87

Table 4.8 Experimental results of all triplicates and standard deviation (for methyl orange under visible light)

Catalyst	Time (hr)	Absorbance			Average absorbance	Standard deviation
		Exp-1	Exp-2	Exp-3		
TiO$_2$ nanoparticles	1	0.66	0.64	0.62	0.64	± 0.02
	2	0.62	0.59	0.53	0.58	± 0.04
	3	0.58	0.52	0.49	0.53	± 0.04
	4	0.56	0.47	0.44	0.49	± 0.06
	5	0.49	0.44	0.42	0.45	± 0.04
N-TiO$_2$	1	0.64	0.63	0.61	0.62	± 0.02
	2	0.56	0.54	0.50	0.53	± 0.03
	3	0.50	0.43	0.42	0.46	± 0.04
	4	0.45	0.39	0.40	0.41	± 0.03
	5	0.37	0.33	0.28	0.32	± 0.04
CoN-TiO$_2$-1	1	0.63	0.58	0.55	0.59	± 0.04
	2	0.55	0.48	0.44	0.49	± 0.05
	3	0.49	0.40	0.38	0.42	± 0.06
	4	0.39	0.37	0.34	0.36	± 0.02
	5	0.29	0.27	0.23	0.26	± 0.03
CoN-TiO$_2$-2	1	0.58	0.57	0.55	0.57	± 0.02
	2	0.47	0.46	0.45	0.46	± 0.01
	3	0.39	0.37	0.35	0.37	± 0.02
	4	0.35	0.33	0.29	0.32	± 0.03
	5	0.20	0.22	0.24	0.22	± 0.02
	1	0.57	0.55	0.51	0.54	± 0.03
	2	0.48	0.45	0.40	0.44	± 0.04

Catalyst	Time					
CoN-TiO$_2$-3	3	0.38	0.35	0.33	0.35	± 0.02
	4	0.30	0.28	0.26	0.28	± 0.02
	5	0.16	0.19	0.22	0.19	± 0.03
CoN-TiO$_2$-4	1	0.55	0.53	0.51	0.53	± 0.02
	2	0.41	0.40	0.38	0.39	± 0.02
	3	0.35	0.33	0.28	0.32	± 0.04
	4	0.25	0.23	0.21	0.23	± 0.02
	5	0.13	0.15	0.17	0.15	± 0.02
CoN-TiO$_2$-5	1	0.47	0.45	0.43	0.45	± 0.02
	2	0.32	0.31	0.30	0.31	± 0.01
	3	0.29	0.25	0.23	0.26	± 0.03
	4	0.15	0.17	0.19	0.17	± 0.02
	5	0.09	0.1	0.14	0.11	± 0.03

Table 4.9 Degradation rate calculation for methyl orange from the absorbance recorded (in visible light)

Catalyst	Time (hr)	Absorbance	C_t	C_o	C_t/C_o	ln C_t/C_o	Negative of ln C_t/C_o
NC-1	1	0.078	0.56		0.86	- 0.15	0.15
	2	0.056	0.52		0.8	- 0.22	0.22
	3	0.044	0.5	0.65	0.76	- 0.27	0.27
	4	0.031	0.47		0.72	- 0.32	0.32
	5	0.015	0.44		0.68	- 0.38	0.38
NC-2	1	0.074	0.56		0.9	- 0.08	0.08
	2	0.055	0.52		0.85	- 0.16	0.16
	3	0.042	0.49	0.61	0.8	- 0.22	0.22
	4	0.022	0.45		0.75	- 0.28	0.28
	5	0.006	0.43		0.70	- 0.36	0.36
NC-3	1	0.080	0.57		0.85	- 0.16	0.16
	2	0.060	0.53		0.79	- 0.24	0.24
	3	0.044	0.50	0.67	0.75	- 0.29	0.29
	4	0.03	0.47		0.7	- 0.36	0.36
	5	0.020	0.45		0.67	- 0.40	0.40

Table 4.10 Experimental results of all triplicates and its standard deviation (for methyl orange under visible light)

Catalyst	Time (hr)	Absorbance			Average absorbance	Standard deviation
		Exp-1	Exp-2	Exp-3		
NC-1	1	0.075	0.078	0.080	0.078	± 0.002
	2	0.053	0.056	0.059	0.056	± 0.003
	3	0.041	0.043	0.048	0.044	± 0.004
	4	0.029	0.031	0.033	0.031	± 0.002
	5	0.013	0.015	0.018	0.015	± 0.003
NC-2	1	0.072	0.074	0.076	0.074	± 0.002
	2	0.052	0.055	0.058	0.055	± 0.003
	3	0.039	0.043	0.044	0.042	± 0.003
	4	0.02	0.021	0.025	0.022	± 0.003
	5	0.004	0.006	0.008	0.006	± 0.002
NC-3	1	0.077	0.081	0.082	0.080	± 0.003
	2	0.058	0.060	0.062	0.060	± 0.002
	3	0.041	0.045	0.046	0.044	± 0.003
	4	0.028	0.029	0.033	0.03	± 0.003
	5	0.018	0.020	0.022	0.020	± 0.002

Order of reaction was determined by plotting a graph between ln Ct/Co and time. The linearity of graph shows that the reaction is of pseudo first order. The order of reaction is also determined from slope of the graph.
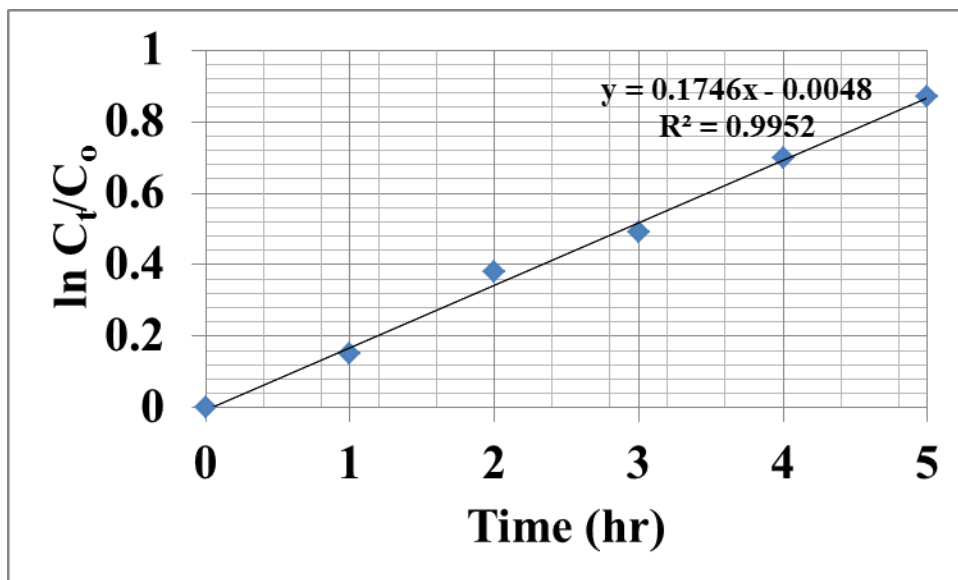
Figure 4.43 Plot between C_t/C_o vs time for methyl orange degradation by using CoN-TiO$_2$-5
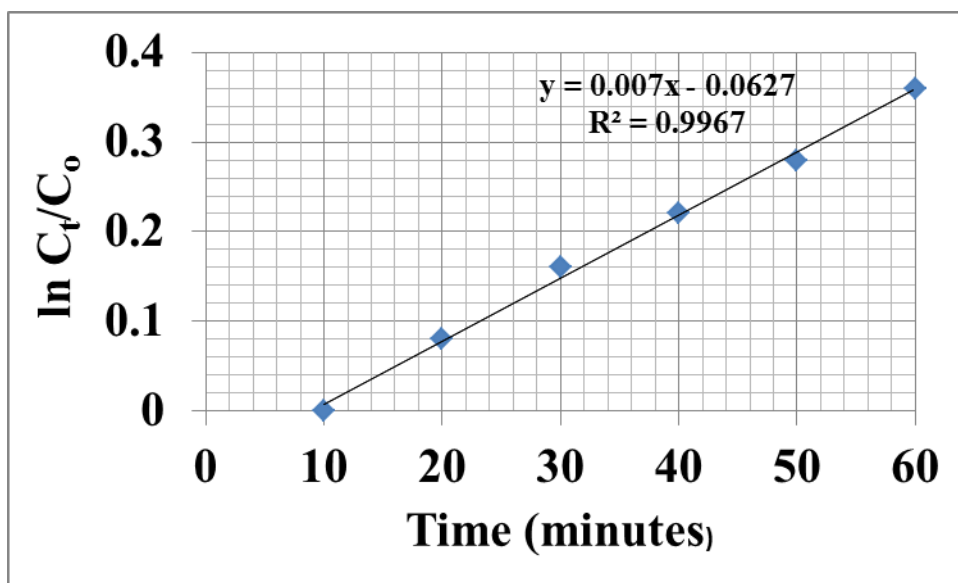
Figure 4.44 Plot between C_t/C_o vs time for methyl orange degradation by using NC-2

Conclusions and Future Plan

Undoped and doped TiO_2 nanoparticles were synthesized by sol-gel method. TTIP, 2-propanol were used as precursors for the synthesis of TiO_2 nanoparticles. Urea and cobalt nitrate were used to dope TiO_2 with nitrogen and cobalt. The synthesized samples were calcined in a muffle furnace at 450°C. The ratio of nitrogen was fixed for all catalysts whereas cobalt doping was carried out in different ratios. All the catalysts were characterized by XRD, SEM, EDX, DRS and BET. XRD analysis showed that anatase was the dominant phase in all samples. SEM analysis showed that all the nanoparticles had spherical morphology and there was significant reduction in particles size after doping and co-doping. BET analysis showed an increase in surface area after co-doping. Along with that UV-DRS results showed significant reduction in band gap after doping and co-doping.

Graphene oxide was also synthesized by using Hummers' method and was characterized by different techniques as well. All the synthesized catalysts were used for the photodegradation of methyl orange. CoN-TiO_2-5 showed highest degradation efficiency of 80% among all the doped catalysts. CoN-TiO_2-5 was selected for the synthesis of nanocomposite with graphene oxide in three different ratios which were 1:1, 1:1.5 and 1:2. These nanocomposites were synthesized by hydrothermal method and were used for the photodegradation of methyl orange. Nanocomposite with 1:1.5 showed highest degradation efficiency of 93%.

In future, these catalysts will be used for the photodegradation of pesticides. Effect of different parameters e.g. dyes concentration, catalyst concentration and effect of pH will be determined. Experiments will also be carried out to determine the optimum concentration of nitrogen, cobalt co-doped TiO_2.

References

[1] D. Vollath, *Nanomaterials*, 2nd ed. Wiley-VCH, 2013, pp. 12-16.

[2] Edelstein and R. Cammarata, *Nanomaterials: synthesis, properties and applications,* Bristol: Institute of Physics Pub, 1996.

[3] N. Kumar and S. Kumbhat, *Essentials in nanoscience and nanotechnology.* John Wiley & Sons, 2016, pp. 30-49.

[4] M. Ashby, P. Ferreira and D. Schodek, *Nanomaterials, nanotechnologies and design*. Butterworth-Heinemann, 2009, pp. 10-15.

[5] Z. Abdullaeva*, Classification of Nanomaterials. Nano and Biomaterials: Compounds, Properties, Characterization, and Applications*. John Wiley & Sons, 2007, pp. 27-56.

[6] G. Fryxell and G. Cao, *Environmental applications of nanomaterials*, 2nd ed. World Scientific, 2012, pp. 3-9.

[7] L. Zheng, F. Hong, S. Lu & C. Liu, "Effect of nano-TiO_2 on strength of naturally aged seeds and growth of spinach", *Biological Trace Element Research*, vol. 104, no. 1, pp. 83-91, 2005.

[8] X. Chen and S. Mao, "Titanium Dioxide Nanomaterials: Synthesis, Properties, Modifications, and Applications", *ChemInform*, vol. 38, no. 41, 2007.

[9] D. Robert, "Photosensitization of TiO_2 by M_xO_y and M_xS_y nanoparticles for heterogeneous photocatalysis applications", *Catalysis Today*, vol. 122, no. 1-2, pp. 20-26, 2007.

[10] FUJISHIMA and K. HONDA, "Electrochemical Photolysis of Water at a Semiconductor Electrode", *Nature*, vol. 238, no. 5358, pp. 37-38, 1972.

[11] P. Amornpitoksuk, S. Suwanboon, S. Sangkanu, A. Sukhoom, N. Muensit and J. Baltrusaitis, "Synthesis, characterization, photocatalytic and antibacterial activities of Ag-doped ZnO powders modified with a diblock copolymer", *Powder Technology*, vol. 219, pp. 158-164, 2017.

[12] S. Hayden, N. Allam and M. El-Sayed, "TiO_2 Nanotube/CdS Hybrid Electrodes: Extraordinary Enhancement in the Inactivation of Escherichia coli", *Journal of the American Chemical Society*, vol. 132, no. 41, pp. 14406–14408, 2017.

[13] D. Tryk, A. Fujishima and K. Honda, "Recent topics in photoelectrochemistry: achievements and future prospects", *Electrochimica Acta*, vol. 45, no. 15-16, pp. 2363-2376, 2000.

[14] M. Grätzel, "Perspectives for dye-sensitized nanocrystalline solar cells", *Progress in Photovoltaics: Research and Applications*, vol. 8, no. 1, pp. 171-185, 2000.

[15] X. CHEN, "Titanium Dioxide Nanomaterials and Their Energy Applications", *Chinese Journal of Catalysis*, vol. 30, no. 8, pp. 839-851, 2009.

[16] B. Tan and Y. Wu, "Dye-Sensitized Solar Cells Based on Anatase TiO_2 Nanoparticle/Nanowire Composites", *The Journal of Physical Chemistry B*, vol. 110, no. 32, pp. 15932-15938, 2006.

[17] T. Lindgren, J. Mwabora, E. Avendaño, J. Jonsson, A. Hoel, C. Granqvist and S. Lindquist, "Photoelectrochemical and Optical Properties of Nitrogen Doped Titanium Dioxide Films Prepared by Reactive DC Magnetron Sputtering", *The Journal of Physical Chemistry B*, vol. 107, no. 24, pp. 5709-5716, 2003.

[18] K. Ho and K. Yeung, "Properties of TiO_2 support and the performance of Au/TiO_2 Catalyst for CO oxidation reaction", *Gold Bulletin*, vol. 40, no. 1, pp. 15-30, 2007.

[19] C. Vayenas, "Heterogeneous catalysis in industrial practice, second edition", *Journal of Catalysis*, vol. 134, no. 2, pp. 755-755, 1992.

[20] F. Boccuzzi, A. Chiorino, S. Tsubota and M. Haruta, "FTIR Study of Carbon Monoxide Oxidation and Scrambling at Room Temperature over Gold Supported on ZnO and TiO_2 2*", The Journal of Physical Chemistry*, vol. 100, no. 9, pp. 3625-3631, 1996.

[21] M. Malekshahi Byranvand, A. Nemati Kharat, L. Fatholahi & Z. Malekshahi Beiranvand, "A review on synthesis of nano-TiO_2 via different methods", *Journal of Nanostructures*, vol. 3, no. 1, pp. 1-9, 2013.

[22] J. H. Braun, A. Baidins & R.E. Marganski, "TiO_2 pigment technology: a review", *Progress in Organic Coatings*, vol. 20, no. 2, pp. 105-138, 1992.

[23] M. Khan, S. Adil and A. Al-Mayouf, "Metal oxides as photocatalysts", *Journal of Saudi Chemical Society*, vol. 19, no. 5, pp. 462-464, 2015.

[24] A. Mills, S. Lee, A. Lepre, I. Parkin and S. O'Neill, "Spectral and photocatalytic characteristics of TiO_2 CVD films on quartz", *Photochemical & Photobiological Sciences*, vol. 1, no. 11, pp.865-868 2017.

[25] B. Ohtani, Y. Ogawa and S. Nishimoto, "Photocatalytic Activity of Amorphous−Anatase Mixture of Titanium(IV) Oxide Particles Suspended in Aqueous Solutions", *The Journal of Physical Chemistry B*, vol. 101, no. 19, pp. 3746-3752, 1997.

[26] M. Batzill, E.H. Morales, & U. Diebold, "Influence of nitrogen doping on the defect formation and surface properties of TiO_2 rutile and anatase", *Physical Review Letters*, vol.96, no.2 026103.

[27] K. Sun, Z. H. Li, "Preparations, properties and applications of chitosan based nanofibers fabricated by electrospinning", *Express Polymer Letters*, vol.5, n0.4, pp. 342–361, 2011.

[28] A.L. Linsebigler, G. Lu, & J.T. Yates, "Photocatalysis on TiO_2 surfaces: principles, mechanisms, and selected results", *Chemical Reviews*, vol. 95, no. 3 pp. 735-758, 1995.

[29] J. Xiao, T. Peng, R. Li, Z. Peng, & C. Yan, "Preparation, phase transformation and photocatalytic activities of cerium-doped mesoporous titania nanoparticles", *Journal of Solid State Chemistry,* vol. 179, no. 4, pp.1161-1170, 2006.

[30] A.R. Ocwelwang. "Photocatalytic Activity and Antibacterial Properties of Ag/N-doped TiO_2 Nanoparticles on PVAE-CS Nanofibre Support" Doctoral dissertation, University of Fort Hare, 2012.

[31] K.S. Novoselov, A.K. Geim, S.V. Morozov, D. Jiang, Y. Zhang, S.V. Dubonos & A.A. Firsov, "Electric field effect in atomically thin carbon films", *Science*, vol.306, no. 5696, pp.666-669, 2004.

[32] C. Lee, X. Wei, J.W. Kysar & J. Hone, J, "Measurement of the elastic properties and intrinsic strength of monolayer graphene", *Science*, vol. 321, no. 5887, pp.385-388, 2008.

[33] J.H. Chen, C. Jang, S. Xiao, M. Ishigami & M.S. Fuhrer, "Intrinsic and extrinsic performance limits of graphene devices on SiO_2", *Nature Nanotechnology*, vol. 3, no. 4, pp. 206-209, 2008.

[34] A.B. Kuzmenko, et al, "Universal optical conductance of graphite", *Physical Review. Letters*, vol. 100, no. 11, 2008.

[35] S. Ghosh, W. Bao, D.L. Nika, S. Subrina, E.P. Pokatilov, C.N. Lau & A.A. Balandin, "Dimensional crossover of thermal transport in few-layer graphene materials", *Nature Materials*, vol.9, pp. 555, 2010.

[36] C.G. Navarro, J.C. Meyer, R.S. Sundaram, A. Chuvilin, S. Kurasch, M. Burghard & U. Kaiser , "Atomic structure of reduced graphene oxide". *Nano Letters*, vol. 10, no. 4, pp. 1144-1148, 2010.

[37] K.A. Mkhoyan, A.W. Contryman, J. Silcox, D.A. Stewart, G. Eda, C. Mattevi & M. Chhowalla, "Atomic and electronic structure of graphene-oxide", *Nano Letters*, vol. 9, no. 3, pp. 1058-1063, 2009.

[38] O.C. Compton, B. Jain, D.A. Dikin, A. Abouimrane, K. Amine & S.T. Nguyen, "Chemically active reduced graphene oxide with tunable C/O ratios", *ACS Nano*, vol. 5, no. 6, pp. 4380-4391, 2011.

[39] D.R. Dreyer, S. Park, C.W. Bielawski & R.S. Ruoff, "The chemistry of graphene oxide", *Chemical Society Reviews*, vol. 39, no. 1, pp. 228- 240, 2010.

[40] C. Mattevi, G. Eda, S. Agnoli, S. Miller, K.A. Mkhoyan, O. Celik, O, & M. Chhowalla, M, "Evolution of electrical, chemical, and structural properties of transparent and conducting chemically derived graphene thin films", *Advanced Functional Materials*, vol. 19, no. 16, pp. 2577-2583, 2009.

[41] W. Choi, I. Lahiri, R. Seelaboyina & Y.S. Kang, "Synthesis of graphene and its applications: a review", *Critical Reviews in Solid State and Materials Sciences*, vol. 35, no. 1, pp. 52-71, 2010.

[42] F. Schedin, A.K. Geim, S.V. Morozov, E.W. Hill, P. Blake, K.S. Novoselov, *Nat. Mater*, vol. 6, pp.652-655.

[43] I. Jung, D.A. Dikin, R.D. Piner & R.S. Ruoff, "Tunable electrical conductivity of individual graphene oxide sheets reduced at "low" temperatures" *Nano Letters*, vol. 8, no. 12, pp. 4283-4287, 2008.

[44] C. Lee, X. Wei, .J.W. Kysar & J. Hone, "Measurement of the elastic properties and intrinsic strength of monolayer graphene", *Science*, vol. 321, no. 5887, pp. 385-388, 2008.

[45] J.W. Suk, R.D. Piner, R. D. J. An & R.S. Ruoff, "Mechanical properties of monolayer graphene oxide", *ACS nano*, vol. 4, no. 11, pp. 6557-6564, 2010.

[46] Q. Zheng, Y. Geng, S. Wang, Z. Li & J.K. Kim, "Effects of functional groups on the mechanical and wrinkling properties of graphene sheets", *Carbon*, vol. 48, no. 15, pp. 4315-4322, 2010.

[47] K.V. Voitko, R.L. Whitby, V.M. Gun'ko, O.M. Bakalinska, M.T. Kartel, K. Laszlo & S.V. Mikhalovsky, "Morphological and chemical features of nano and macroscale carbons affecting hydrogen peroxide decomposition in aqueous media", *Journal of Colloid and Interface Science*, vol. 361, no. 1, pp. 129-136, 2011.

[48] D.R. Dreyer, S. Park, C.W. Bielawski & R.S. Ruoff, "The chemistry of graphene oxide", *Chemical Society Reviews*, vol. 39, no. 1, pp. 228-240, 2010.

[49] C. Su & K.P Loh, "Carbocatalysts: graphene oxide and its derivatives", *Accounts of Chemical Research*, vol. 46, no. 10, pp. 2275-2285, 2012.

[50] G.K. Ramesha, A.V. Kumara, H.B. Muralidhara & S. Sampath, "Graphene and graphene oxide as effective adsorbents toward anionic and cationic dyes", *Journal of Colloid and Interface Science*, vol. 361, no. 1, pp. 270-277, 2011.

[51] M.Z. Kassaee, E. Motamedi & M. Majdi, "Magnetic Fe_3O_4-graphene oxide/polystyrene: fabrication and characterization of a promising nanocomposite", *Chemical Engineering Journal*, vol. 172, no. 1, pp. 540-549, 2011.

[52] X. Zhou, Y. Zhang, C. Wang, X. Wu, Y. Yang, B. Zheng & J. Zhang, "Photo-Fenton reaction of graphene oxide: a new strategy to prepare graphene quantum dots for DNA cleavage", *Acs Nano*, vol. 6, no. 8, pp. 6592-6599, 2012.

[53] A. Bagri, C. Mattevi, M. Acik, Y.J. habal, M. Chhowalla & V.B. Shenoy, "Structural evolution during the reduction of chemically derived graphene oxide", *Nature Chemistry*, vol. 2, issue. 7, pp. 581-587, 2010.

[54] J. Hou, Z. Wang, W. Kan, S. Jiao, H. Zhu & R.V. Kumar. "Efficient visible-light-driven photocatalytic hydrogen production using CdS@ TaON core–shell composites coupled with graphene oxide nanosheets", *Journal of Materials Chemistry*, vol. 22, no. 15, pp. 7291-7299, 2012.

[55] J. Bian, M. Xiao, S.J. Wang, Y.X. Lu & Y.Z. Meng, "Graphite oxide as a novel host material of catalytically active Cu–Ni bimetallic nanoparticles", *Catalysis Communications*, vol. 10, no. 11, pp. 1529-1533, 2009.

[56] F. Bei, X. Hou, S.L. Chang, G.P. Simon & D. Li, "Interfacing colloidal graphene oxide sheets with gold nanoparticles", *Chemistry-A European Journal*, vol. 17, no. 21, pp. 5958-5964, 2011.

[57] W. Lu, R. Ning, X. Qin, Y. Zhang, G. Chang, S. Liu, & X. Sun, "Synthesis of Au nanoparticles decorated graphene oxide nanosheets: Noncovalent functionalization by TWEEN 20 in situ reduction of aqueous chloroaurate ions for hydrazine detection and catalytic reduction of 4-nitrophenol", *Journal of Hazardous Materials*, vol. 197, pp. 320-326, 2011.

[58] J. Jeyaratnam, "Health problems of pesticide usage in the Third World", *British Journal of Industrial Medicine*, vol. 42, no. 8, pp. 503- 505, 1985.

[59] G. Potashnik & A. Porath, "Dibromochloropropane (DBCP): a 17-year reassessment of testicular function and reproductive performance", *Journal of Occupational and Environmental Medicine*, vol. 37, no. 11, pp. 1287-1292, 1995.

[60] A. Gupta, D.K. Rai, R.S. Pandey B. & Sharma, "Analysis of some heavy metals in the riverine water, sediments and fish from river Ganges at Allahabad", *Environmental Monitoring and Assessment*, vol. 157, no. 1, pp. 449- 458, 2009.

[61] A. Agrawal, R.S. Pandey & B. Sharma, "Water pollution with special reference to pesticide contamination in India", *Journal of Water Resource and Protection*, vol. 2, no. 5, pp. 432, 2010.

[62] S.O. Igbedioh, "Effects of agricultural pesticides on humans, animals, and higher plants in developing countries", *Archives of Environmental Health: An International Journal*, vol. 46, no. 4, pp. 218-224, 1991.

[63] P.B. Bedient, H.S. Rifai, H. S & C.J. Newell, "Ground water contamination: transport and remediation", *Prentice-Hall International*, 2011.

[64] H.L. Bradlow, D.L. Davis, G. Lin, D. Sepkovic, D & R. Tiwari, "Effects of pesticides on the ratio of 16 alpha/ 2-hydroxyestrone: a biologic marker of breast cancer risk", *Environmental Health Perspectives*, vol. 103, no.7, pp. 147, 1995.

[65] S. Netpradit, P. Thiravetyan & S. Towprayoon, "Adsorption of three azo reactive dyes by metal hydroxide sludge: effect of temperature, pH, and electrolytes", *Journal of Colloid and Interface Science*, vol. 270, no. 2, pp. 255-261, 2004.

[66] A.E. Ghaly, R. Ananthashankar, M.V. Alhattab & V.V. Ramakrishnan, "Production, characterization and treatment of textile effluents: a critical review", *Journal of Chemical Engineering & Process Technology*, vol. 5, no.1, 2014.

[67] R.O.A. de Lima, A.P. Bazo, D.M.F. Salvadori, C.M. Rech, C. M, D. Palma Oliveira & G. de Aragão Umbuzeiro, "Mutagenic and carcinogenic potential of a textile azo dye processing

plant effluent that impacts a drinking water source", *Mutation Research/Genetic Toxicology and Environmental Mutagenesis*, vol. 626, no. 1, pp. 53-60, 2007.

[68] F.M.D. Chequer, G.A.R. de Oliveira, E.R.A. Ferraz, J.C. Cardoso, M.V.B. Zanoni & D.P. de Oliveira, 'Textile dyes: dyeing process and environmental impact", *In Eco-Friendly Textile Dyeing and Finishing*, 2013.

[69] S. Pişkin, S. Kasap & M. Sari Yılmaz, "Synthesis of TiO_2 nanoparticles by sol-gel and sonochemical combination", *International Journal of Chemical and Molecular Engineering*, vol. 3, no. 1, 2016.

[70] P.S. Shinde & C.H. Bhosale, "Properties of chemical vapour deposited nanocrystalline TiO_2 thin films and their use in dye-sensitized solar cells", *Journal of Analytical and Applied Pyrolysis*, vol. 82, no. 1, pp. 83-88, 2008.

[71] J. Choi, H. Park & M.R. Hoffmann, "Effects of single metal-ion doping on the visible-light photoreactivity of TiO_2", *The Journal of Physical Chemistry C*, vol. 114, no. 2, pp. 783-792, 2009.

[72] W.C. Hao, S.K. Zheng, C. Wang & T.M. Wang, "Comparison of the photocatalytic activity of TiO_2 powder with different particle size", *Journal of Materials Science Letters*, vol. 21, no. 20, pp. 1627-1629, 2002.

[73] C.S. Kim, K. Nakaso, B. Xia, K. Okuyama & M. Shimada, "A new observation on the phase transformation of TiO_2 nanoparticles produced by a CVD method", *Aerosol Science and Technology*, vol. 39, no. 2, pp. 104-112, 2005.

[74] P. S. Shinde & C.H. Bhosale, "Properties of chemical vapour deposited nanocrystalline TiO_2 thin films and their use in dye-sensitized solar cells", *Journal of Analytical and Applied Pyrolysis*, vol. 82, no. 1, pp. 83-88, 2008.

[75] T. Sugimoto, K. Okada & H. Itoh, "Synthetic of uniform spindle-type titania particles by the gel–sol method", *Journal of Colloid and Interface Science*, vol. 193, no. 1, pp. 140-143, 1997.

[76] H.S. Jahromi, H. Taghdisian, S. Afshar & S. Tasharrofi, "Effects of pH and polyethylene glycol on surface morphology of TiO_2 thin film", *Surface and Coatings Technology*, vol. 203, no. 14, pp. 1991-1996, 2009.

[77] D. Vorkapic & T. Matsoukas, "Effect of temperature and alcohols in the preparation of titania nanoparticles from alkoxides", *Journal of the American Ceramic Society*, vol. 81, no. 11, pp. 2815-2820, 1998.

[78] Y.T. Moon, H.K. Park, D.K. Kim, C.H. Kim & I.S. Seog, "Preparation of monodisperse and spherical zirconia powders by heating of alcohol–aqueous salt solutions", *Journal of the American Ceramic Society*, vol. 78, no. 10, pp. 2690-2694, 1995.

[79] M. A. Behnajady, H. Eskandarloo, N. Modirshahla, & Shokri, "Investigation of the effect of sol–gel synthesis variables on structural and photocatalytic properties of TiO_2 nanoparticles", *Desalination*, vol. 278, no. 1, pp. 10-17, 2011.

[80] Y. Xu, W. Zheng & W. Liu, "Enhanced photocatalytic activity of supported TiO_2: dispersing effect of SiO_2", *Journal of Photochemistry and Photobiology A: Chemistry*, vol. 122, no. 1, 57-60, 1999.

[81] M. Pal, J. Garcia Serrano, P. Santiago & U. Pal, "Size-controlled synthesis of spherical TiO_2 nanoparticles: morphology, crystallization, and phase transition", *The Journal of Physical Chemistry C*, vol. 111, no. 1, pp. 96-102, 2007.

[82] X. Chen, & S.S. Mao, "Titanium dioxide nanomaterials: synthesis, properties, modifications, and applications", *Chem. Rev*, vol. 107, no. 7, pp. 2891-2959, 2007.

[83] X. Wang, J.C. Yu, Y. Chen, L. Wu & X. Fu, "ZrO_2-Modified Mesoporous Nanocrystalline TiO_2-x Nx as Efficient Visible Light Photocatalysts", *Environmental Science & Technology*, vol. 40, no. 7, pp. 2369-2374, 2006.

[84] T. Tachikawa, M. Fujitsuka & T. Majima, "Mechanistic insight into the TiO_2 photocatalytic reactions: design of new photocatalysts", *The Journal of Physical Chemistry C*, vol. 111, no. 14, pp. 5259-5275, 2007.

[85] A. Kumbhar & G. Chumanov, "Synthesis of iron (III)-doped titania nanoparticles and its application for photodegradation of sulforhodamine-B pollutant", *Journal of Nanoparticle Research*, vol. 7, no. 4, pp. 489-498, 2005.

[86] Y. Cong, J. Zhang, F. Chen, M. Anpo & D. He, "Preparation, photocatalytic activity, and mechanism of nano-TiO_2 co-doped with nitrogen and iron (III)", *The Journal of Physical Chemistry C*, vol. 111, no. 28, pp. 10618-10623, 2007.

[87] T. Morikawa, R. Asahi, T. Ohwaki, K. Aoki, K. Suzuki & Y. Taga, "Visible-light photocatalyst-nitrogen-doped titanium dioxide", *R&D Rev. Toyota CRDL*, vol. 40, pp. 45-50, 2005.

[88] K.T. Ranjit & B. Viswanathan, "Synthesis, characterization and photocatalytic properties of iron-doped TiO$_2$ catalysts", *Journal of Photochemistry and Photobiology A: Chemistry*, vol. 108, no. 1, pp. 79-84, 1997.

[89] C.T. Wang & S.H. Ro, "Nanocluster iron oxide-silica aerogel catalysts for methanol partial oxidation", *Applied Catalysis A: General*, vol. 285, no. 1, pp. 196-204, 2005.

[90] T. J. Kemp & R.A. McIntyre, "Transition metal-doped titanium (IV) dioxide: Characterisation and influence on photodegradation of poly (vinyl chloride)", *Polymer Degradation and Stability*, vol. 91, no. 1, pp. 165-194, 2006.

[91] D.J. Reidy, J.D. Holmes & M.A. Morris, "Preparation of a highly thermally stable titania anatase phase by addition of mixed zirconia and silica dopants", *Ceramics International*, vol. 32, no. 3, pp. 235-239, 2006.

[92] V. Etacheri, C. Di Valentin, J. Schneider, D. Bahnemann & S.C. Pillai, "Visible-light activation of TiO$_2$ photocatalysts: advances in theory and experiments", *Journal of Photochemistry and Photobiology C: Photochemistry Reviews*, vol. 25, pp. 1-29, 2015.

[93] W. Choi, A. Termin & M.R. Hoffmann, "The role of metal ion dopants in quantum-sized TiO$_2$: correlation between photoreactivity and charge carrier recombination dynamics", *The Journal of Physical Chemistry*, vol. 98, no. 51, pp. 13669-13679, 1994.

[94] A. Di Paola, G. Marci, L. Palmisano, M. Schiavello, K. Uosaki, S. Ikeda & B. Ohtani, "Preparation of polycrystalline TiO$_2$ photocatalysts impregnated with various transition metal ions: characterization and photocatalytic activity for the degradation of 4-nitrophenol", *The Journal of Physical Chemistry B*, vol. 106, no. 3, pp. 637-645, 2002.

[95] R.Y. O. J. I. Asahi, T.A.K.E.S. H.I. Morikawa, T. Ohwaki, T, K. Aoki, K & Y. Taga, "Visible-light photocatalysis in nitrogen-doped titanium oxides", *Science*, vol. 293, no. 5528, pp. 269-271, 2001.

[96] R. Asahi, T. Morikawa, H. Irie & T. Ohwaki, "Nitrogen-doped titanium dioxide as visible-light-sensitive photocatalyst: designs, developments, and prospects", *Chemical Reviews*, vol. 114, no. 19, pp. 9824-9852, 2014.

[97] H. Li, Y. Hao, H. Lu, L. Liang, Y. Wang, J. Qiu & J. Yao, "A systematic study on visible-light N-doped TiO$_2$ photocatalyst obtained from ethylenediamine by sol–gel method", *Applied Surface Science*, vol. 344, pp. 112-118, 2015.

[98] X. Chen, L. Liu, Y.Y. Peter & S.S. Mao, "Increasing solar absorption for photocatalysis with black hydrogenated titanium dioxide nanocrystals", *Science*, vol. 331, no. 6018, pp.746-750, 2011.

[99] T. Ohno & N. Mukawa, "A free-head, simple calibration, gaze tracking system that enables gaze-based interaction", *In Proceedings of the 2004 symposium on Eye tracking research and applications*, 2004, pp. 115-122.

[100] J.C. Yu, J. Yu, W. Ho, Z. Jiang & L. Zhang, "Effects of F-doping on the photocatalytic activity and microstructures of nanocrystalline TiO_2 powders", *Chemistry of Materials*, vol. 14, no. 9, pp. 3808-3816, 2002.

[101] T.M. Breault & B.M. Bartlett, "Lowering the band gap of anatase-structured TiO_2 by coalloying with Nb and N: electronic structure and photocatalytic degradation of methylene blue dye", *The Journal of Physical Chemistry C*, vol. 116, no. 10, pp. 5986–5994, 2012.

[102] X. Li, Q. Liu, X. Jiang & J. Huang, "Enhanced photocatalytic activity of Ga-N Co-doped anatase TiO_2 for water decomposition to hydrogen", *Int J Electrochem Sci*, vol. 7, pp. 11519-11527, 2012.

[103] Y. Li & Z. Yu, "Multiple shared trees multicast based on set covering and Ant Colony Optimization. In Consumer Electronics, Communications and Networks (CECNet)", 2nd International Conference on, pp. 391-393, 2012.

[104] M. Feilizadeh, M. Vossoughi, S.M.E. Zakeri & M. Rahimi, "Enhancement of efficient Ag–S/TiO_2 nanophotocatalyst for photocatalytic degradation under visible light", *Industrial & Engineering Chemistry Research*, vol. 53, no. 23, pp. 9578-9586, 2014.

[105] D. Dolat, S. Mozia, B. Ohtani & A.W. Morawski, "Nitrogen, iron-single modified (N-TiO_2, Fe-TiO_2) and co-modified (Fe, N-TiO_2) rutile titanium dioxide as visible-light active photocatalysts", *Chemical Engineering Journal*, vol. 225, pp. 358-364, 2013.

[106] S. Liu, X. Sun, .J.G. Li, X. Li, Z. Xiu, H. Yang & X. Xue, "Fluorine-and iron-modified hierarchical anatase microsphere photocatalyst for water cleaning: facile wet chemical synthesis and wavelength-sensitive photocatalytic reactivity", *Langmuir*, vol. 26, no. 6, pp. 4546-4553, 2009.

[107] X. Jiang, Y. Zhang, J. Jiang, Y. Rong, Y. Wang, Y. Wu & C. Pan, "Characterization of oxygen vacancy associates within hydrogenated TiO_2: a positron annihilation study", *The Journal of Physical Chemistry C*, vol. 116, no. 42, pp. 22619-22624, 2012.

[108] J. Wang, Y.F. Zhao, T. Wang, H. Li & C. Li, "Photonic, and photocatalytic behavior of TiO_2 mediated by Fe, CO, Ni, N doping and co-doping", *Physica B: Condensed Matter*, vol. 478, pp. 6-11, 2011.

[109] S.G. Yan & J.T. Hupp, "Semiconductor-based interfacial electron-transfer reactivity: decoupling kinetics from pH-dependent band energetics in a dye-sensitized titanium dioxide/aqueous solution system", *The Journal of Physical Chemistry*, vol. 100, no. 17, pp. 6867-6870, 1996.

[110] K. Gurunathan, P. Maruthamuthu & M.V.C. Sastri, "Photocatalytic hydrogen production by dye-sensitized Pt/SnO_2 and $Pt/SnO_2/RuO_2$ in aqueous methyl viologen solution", *International Journal of Hydrogen Energy*, vol. 22, no. 1, pp. 57-62, 1997.

[111] R.A. Doong, C. H. Chen, R.A. Maithreepala & S.M. Chang, "The influence of pH and cadmium sulfide on the photocatalytic degradation of 2-chlorophenol in titanium dioxide suspensions", *Water Research*, vol. 35, no. 12, pp. 2873- 2880, 2011.

[112] V. Keller & F. Garin, "Photocatalytic behavior of a new composite ternary system: $WO_3/SiC-TiO_2$. Effect of the coupling of semiconductors and oxides in photocatalytic oxidation of methylethylketone in the gas phase", *Catalysis Communications*, vol. 4, no. 8, pp. 377-383, 2003.

[113] D. Wang, R. Kou, D. Choi, Z. Yang, Z. Nie, J. Li & J. Liu, "Ternary self-assembly of ordered metal oxide- graphene nanocomposites for electrochemical energy storage", *ACS nano*, vol. 4, no. 3, pp. 1587-1595, 2010.

[114] D. Maruthamani, D. Divakar & M. Kumaravel, "Enhanced photocatalytic activity of TiO_2 by reduced graphene oxide in mineralization of Rhodamine B dye", *Journal of Industrial and Engineering Chemistry*, vol. 30, pp. 33-43, 2015.

[115] S. H. Park & J. Bae, "Tailoring environment friendly carbon nanostructures by surfactant mediated interfacial engineering", *Journal of Industrial and Engineering Chemistry*, vol. 30, pp. 1-9, 2015.

[116] P. Gao, A. Li, D. D. Sun & W .J. Ng, "Effects of various TiO_2 nanostructures and graphene oxide on photocatalytic activity of TiO_2", *Journal of Hazardous Materials*, vol. 279, pp. 96-104, 2014.

[117] H. M. Yadav & J. S. Kim, "Solvothermal synthesis of anatase TiO_2-graphene oxide nanocomposites and their photocatalytic performance", *Journal of Alloys and Compounds*, vol. 688, pp. 123-129, 2016.

[118] V. Štengl, S. Bakardjieva, T. M. Grygar, J. Bludská & M. Kormunda, "TiO_2-graphene oxide nanocomposite as advanced photocatalytic materials", *Chemistry Central Journal*, vol. 7, no. 1, pp. 41, 2013.

[119] L. R. Narayana, M. Matheswaran, A. A. Aziz & P. Saravanan, "Photocatalytic decolourization of basic green dyes by pure and Fe, Co doped TiO_2 under daylight illumination", *Desalination*, vol. 269, no. 1, pp. 249-253, 2011.

[120] L. Patterson, "The Scherrer formula for X-ray particle size determination", *Physical Review*, vol. 56, no. 10, pp. 978, 1939.

[121] Basheer, "Application of titanium dioxide-graphene composite material for photocatalytic degradation of alkyl phenols", *Journal of Chemistry*, vol. 2013, 2012.

[122] Q. Z. Wen-Yuan Yan, Xing Chen, Xing-Jiu Huang, Yu-Cheng Wu, "C-doped and N-doped reduced graphene oxide/TiO_2 composites with exposed (0 0 1) and (1 0 1) facets controllably synthesized by a hydrothermal route and their gas sensing characteristics", *Sensors and Actuators B*, vol. 230, pp. 761–772, 2016.